10.1161/CIRCULATIONAHA.118.034757

Cystathionine γ lyase Sulfhydrates the RNA Binding Protein HuR to Preserve Endothelial Cell Function and Delay Atherogenesis

Running Title: *Sofia-Iris Bibli & Jiong Hu, et al.; CSE and Human Atherosclerosis*

Sofia-Iris Bibli & Jiong Hu, et al.

The full author list is available on pages 19-20.

Address for Correspondence:
Ingrid Fleming, PhD
Institute for Vascular Signalling
Centre for Molecular Medicine
Goethe University
Theodor Stern Kai 7
60596 Frankfurt am Main, Germany
Tel: +49 69 6301 6972
Email: fleming@em.uni-frankfurt.de

Abstract

Background—Hydrogen sulfide (H_2S), generated by cystathionine γ lyase (CSE), is an important endogenous regulator of vascular function. The aim of the present study was to investigate the control and consequences of CSE activity in endothelial cells under physiological and pro-atherogenic conditions.

Methods—Endothelial cell CSE knock out mice were generated and lung endothelial cells were studied *in vitro* (gene expression, protein sulfhydration and monocyte adhesion). Mice were crossed onto the $ApoE^{-/-}$ background and atherogenesis (partial carotid artery ligation) was monitored over 21 days. CSE expression, H_2S bioavailability and amino acid profiling were also performed using human material.

Results—The endothelial cell-specific deletion of CSE selectively increased the expression of CD62E and elevated monocyte adherence in the absence of an inflammatory stimulus. Mechanistically, CD62E mRNA was more stable in endothelial cells from CSE-deficient mice, an effect attributed to the attenuated sulfhydration and dimerization of the RNA-binding protein HuR. CSE expression was upregulated in mice following partial carotid artery ligation as well as in atheromas from human subjects. Despite the increase in CSE protein, circulating and intra-plaque H_2S levels were reduced, a phenomenon that could be attributed to the serine phosphorylation (on Ser377) and inhibition of the enzyme, most likely due to increased IL-1β. Consistent with the loss of H_2S, HuR sulfhydration was attenuated in atherosclerosis, and resulted in the stabilization of HuR-target mRNAs e.g. CD62E and cathepsin S, both of which are linked with endothelial cell activation and atherosclerosis. The deletion of CSE from endothelial cells was associated with the accelerated development of endothelial dysfunction and atherosclerosis, effects that were reversed upon treatment with a H_2S donor. Finally, in mice and humans, plasma levels of the CSE substrate; L-cystathionine, negatively correlated with vascular reactivity and H_2S levels indicating its potential use as a biomarker for vascular disease.

Conclusions—The constitutive S-sulfhydration of HuR (on Cys13) by CSE-derived H_2S prevents its homo-dimerization and activity which attenuates the expression of target proteins such as CD62E and cathepsin S. However, as a consequence of vascular inflammation the beneficial actions of CSE-derived H_2S are lost due to the phosphorylation and inhibition of the enzyme.

Key Words: Adhesion molecule; Atherogenesis; Biomarker; Hydrogen sulphide; RNA binding protein

Clinical Perspective

What is new?

- Hydrogen sulfide (H_2S) generated by cystathionine γ lyase (CSE) constitutively sulfhydrates the RNA binding protein HuR, to prevent its homo dimerization and attenuate its activity in the vessel wall.
- The sulfhydration of HuR prevents its binding to, and stabilization of, target mRNAs e.g. CD62E (E-selectin) – ensuring their low expression.
- Inflammation results in the phosphorylation and inhibition of CSE, which reduces H_2S production and thus alleviates the inhibition of HuR.
- Endothelial ablation of CSE results in increased CD62E expression and accelerated development of endothelial dysfunction and atherosclerosis.
- Plasma levels of the CSE substrate; L-cystathionine, correlate with impaired vascular reactivity in humans.

What are the clinical implications?

- Oral supplementation with H_2S donors (e.g. SG1002) may serve as a therapeutic approach to attenuate atherosclerosis development in humans.
- Circulating L-cystathionine levels can serve as a biomarker for endothelial dysfunction.

Introduction

Despite intensive therapy, the clinical manifestations of atherosclerosis remain the primary cause of morbidity and mortality worldwide. Atherosclerotic plaque formation mainly occurs at susceptible sites of major arteries in which disturbed flow can activate endothelial cells, leading to altered expression of genes involved in inflammatory process and the development of vascular disease.[1,2] A number of stimuli and factors have been found to be important to maintain endothelial cells in a quiescent and anti-atherogenic state, including the shear stress-stimulated generation of nitric oxide (NO). Apart from NO, there are other gasotransmitters that are thought to play a significant role in vascular homeostasis including carbon monoxide and hydrogen sulfide (H_2S). H_2S is generated mainly via the reverse trans-sulfuration pathway in reactions catalyzed by two pyridoxal phosphate-dependent enzymes i.e., cystathionine-β-synthase (CBS) and cystathionine-γ-lyase (CSE), and one pyridoxal phosphate-independent enzyme i.e. 3-mercaptopyruvate sulfurtransferase (3MST).[3,4] The production of H_2S in the vasculature is largely attributed to the activity of CSE which generates H_2S from L-cysteine and L-cystathionine, and has been implicated in the modulation of angiogenesis and vascular tone.[5] However, the mechanism(s) regulating the expression of CSE in endothelial cells and the molecular targets of CSE-derived H_2S remain to be elucidated.

Even though partially contradictory phenotypes on blood pressure changes and hyper-homocysteinemia have been observed; that seem to depend on the genetic background of the mice studied,[6,7] it seems clear that CSE-derived H_2S can exert anti-atherosclerotic effects.[8-10] In mice lacking CSE, both elevated adhesion molecule levels and enhanced leukocyte adherence have been described,[8] while the overexpression of CSE was found to reduce atherosclerotic plaque size and circulating lipid levels.[11] In humans, CSE has been detected in atherosclerotic

plaques,[12,13] but little is known about its consequences on disease development or outcome. The aims of this study, therefore, were to determine the mechanism(s) by which CSE expression and activity is regulated in endothelial cells and to unravel its potential role in the initiation and development of atherosclerosis in mice and humans. Moreover, as at the molecular level H_2S signals through the persulfidation or sulfhydration of target cysteine residues,[14,15] we set out to identify physiologically relevant sulfhydration targets that may be altered during, and contribute to, disease development.

Methods

Detailed methods are available in the online-only Data Supplement. Requests by researchers to access the data, analytic methods, and study materials for the purposes of reproducing the results or replicating procedures can be made to the corresponding author who manages the information.

Animals

Apolipoprotein E-deficient ($ApoE^{-/-}$) mice were purchased from Charles River Laboratories (Sulzfeld, Germany). Floxed CSE ($CSE^{fl/fl}$) mice were generated as described[7], and crossed with tamoxifen-inducible Cdh5-CreERT2 mice[16] in the C57/BL6J background or with Cdh5-Cre mice in the $ApoE^{-/-}$ background. Mice were housed in conditions that conform to the *Guide for the Care and Use of Laboratory Animals* published by the U.S. National Institutes of Health (NIH publication no. 85-23). Animals received the usual laboratory diet and all studies were approved by the animal research ethics committees in Athens (790/13-02-2014) and Darmstadt (FU1177 and FU1189). Littermates of both genders were used. To induce robust Cre activity, animals were treated with tamoxifen (75 mg/kg i.p., Sigma-Aldrich) for 5 days.

Human samples

Carotid plaques were prospectively collected from 24 random patients, who had internal carotid artery (ICA) stenosis of 75-90% and underwent carotid endarterectomy (**Supplemental Table I**). Arteriographical evaluation of the carotid bifurcation stenosis was performed and the degree of luminal stenosis was determined according to North American Symptomatic Carotid Endarterectomy Trial (NASCET) criteria. Peak systolic velocity was monitored by using a Philips HD11 ultrasound platform (Philips, Netherlands). Eight additional samples of healthy thyroid arteries were used as the control group. Thyroid arteries were chosen from aged matched subjects without additional comorbidities (**Supplemental Table I**). Samples were collected post-mortem and were evaluated by a pathologist for the possibility of atherosclerotic lesions. Arteries that showed no pathological characteristics were snap frozen for additional analysis. Tissue samples were either frozen and used for biochemical analyses or embedded in paraffin for immunostaining. Plasma from a further 70 patients with internal carotid artery stenosis of 75-90% before carotid endarterectomy and 32 age matched healthy donors was used for amino acid profiling, H_2S measurements and assay of IL-1β levels (**Supplemental Table II**). All studies followed the Code of Ethics of the World Medical Association (Declaration of Helsinki). The study protocols were approved by the Institutional Ethics Committee (Scientific and Ethic Committee of Hipokrateion University Hospital, PN1539) and all patients gave their informed consent.

Statistics

Data are expressed as mean ± SEM. Statistical evaluation was performed using Student's t-test for unpaired data. The Mann-Whitney test was used if the sample size was lower than 8 or populations followed non-Gaussian distribution. One-way ANOVA followed by Newman-Keuls

test and two-way ANOVA with a Bonferroni post-test were used where appropriate. The Pearson correlation coefficient was used to measure association between continuous variables. ANOVA repeated measures with a Bonferroni post-test was used where appropriate. Statistical tests are described in the figure legend for each experiment. Central tendency and dispersion of the data were examined for replicates below 6. Values of $P<0.05$ were considered statistically significant. MetaboAnalyst[17] was used to construct the heat map and perform hierarchical clustering based on amino acid profile.

Results

Link between fluid shear stress, CSE expression and CD62E expression

Given that shear stress is a key player in endothelial cell homeostasis and atherosclerosis development, the expression of CSE in endothelial cells along the aorta was assessed, concentrating on potential changes in areas normally associated with high shear stress/laminar flow versus low shear stress/disturbed flow. In contrast to the changes described for the endothelial NO synthase (eNOS),[18,19] the expression of CSE was higher in the lesser curvature and arterial bifurcations and lower in the descending aorta (**Figure 1A&B**), implying that CSE expression was negatively regulated by shear stress. In line with these observations, the application of fluid shear stress to cultured human endothelial cells resulted in a time dependent decrease in CSE protein levels (**Figure 1C&D**), as well as H_2S production (**Figure 1D**). Shear stress did not alter the expression of the other H_2S generating enzymes i.e., CBS and 3MST, in endothelial cells (**Supplemental Figure 1A**).

The importance of CSE in endothelial cell homeostasis was studied in inducible endothelial cell-specific CSE knockout ($CSE^{i\Delta EC}$) mice. Treating $CSE^{i\Delta EC}$ mice with tamoxifen

abrogated CSE expression in endothelial cells and resulted in an approximately 65% reduction in H_2S production (**Figure 1A**, **Supplemental Figure 1B&C**). Interestingly, while intracellular adhesion molecule (ICAM)-1 and vascular cell adhesion molecule (VCAM)-1 were barely detectable in cells from wild-type and $CSE^{i\Delta EC}$ mice (**Supplemental Figure 2A**, **Figure 1E**), the expression of CD62E (E-selectin) was elevated in $CSE^{i\Delta EC}$ endothelial cells, in the absence of any inflammatory stimulus. Similar effects were observed in freshly isolated aortae from wild-type and $CSE^{i\Delta EC}$ mice (**Supplemental Figure 2B**). The increased CD62E in endothelial cells from $CSE^{i\Delta EC}$ mice was functional as it was expressed on the cell surface (**Supplemental Figure 2C**) and correlated with an increase in monocyte adhesion to CSE-deficient endothelial cells under basal conditions (**Supplemental Figure 2D**). Moreover, the increase in monocyte adherence was abrogated in cells treated with a CD62E neutralizing antibody (**Supplemental Figure 2E**). Importantly, rescue experiments, in which CSE was reintroduced into CSE-deficient endothelial cells, suppressed the abnormal CD62E expression and abolished monocyte adhesion (**Supplemental Figure 2F-G**). These effects were unrelated to changes in NO production, as the differences between wild-type and CSE-deficient endothelial cells were unaffected by the addition of a NOS inhibitor (**Supplemental Figure 2H**). Cell stimulation with interleukin (IL)-1β increased ICAM-1, VCAM-1 and CD62E in cells from wild-type mice but failed to further increase CD62E levels in $CSE^{i\Delta EC}$ mice (**Figure 1E**) even though VCAM-1 and ICAM-1 expression and monocyte adherence increased as expected (**Supplemental Figure 2A&B**).

Sulfhydration of HuR by CSE-derived H_2S

The selective upregulation of CD62E in endothelial cells lacking CSE suggested that CD62E may be directly targeted by CSE-derived H_2S. However, it was not possible to demonstrate the sulfhydration of CD62E in CSE-expressing endothelial cells, indicating that the effect was

indirect. Therefore, to identify potential H_2S targets, CSE was immunoprecipitated from murine endothelial cells and co-precipitated proteins identified by mass spectrometry. This procedure revealed that CSE interacts with a number of proteins under basal conditions (**Supplemental Table 3**), including the RNA-binding protein human antigen R (HuR, also known as ELAV-like protein 1) (**Supplemental Figure 3A**). This was relevant inasmuch as CD62E mRNA levels are reportedly regulated by HuR,[20] and CD62E mRNA was more stable in CSE-deficient cells than in CSE expressing cells treated with actinomycin D (**Supplemental Figure 3B**). The association of HuR with CSE could be confirmed by immunoprecipitating the enzyme from CSE-overexpressing endothelial cells (**Figure 2A**).

HuR is an attractive candidate for sulfhydration as it possesses three cysteines, one of which (Cys13) is predicted to be highly nucleophilic and unlikely to remain as a free cysteine (http://clavius.bc.edu/~clotelab/DiANNA; http://propka.org).[21-23] A biotin-thiol labelling assay, revealed the specific, DTT-sensitive sulfhydration of HuR in cells from wild-type mice but not in cells from $CSE^{i\Delta EC}$ mice (**Figure 2B**). Similar results were obtained using a modified *in situ* biotin switch-coupled proximity ligation assay (**Figure 2C**). To identify which cysteine was targeted by H_2S, a series of mutants was generated in which Cys13, Cys245 and Cys284 were replaced by alanine. When introduced into CSE-expressing HEK-293 cells, the wild-type HuR as well as the Cys245Ala and Cys284Ala mutants were sulfhydrated, while the Cys13Ala mutant was not (**Figure 2D**).

One possible consequence of HuR sulfhydration is an alteration in conformation as the dimerization of the two RNA recognition motifs within the HuR protein requires a disulfide bond on Cys13.[24] In agreement with this, the ability of the Cys13Ala HuR mutant to form dimers was impaired (**Figure 2E**). Moreover, in endothelial cells from wild-type mice, HuR was detected in

its monomeric (inactive) and dimeric (active) forms, but only as a dimer in cells from $CSE^{i\Delta EC}$ mice (**Figure 2F**), indicating increased HuR activity in CSE-deficient cells. Indeed, substantially more CD62E mRNA bound to HuR immunoprecipitated from CSE-deficient than CSE-expressing endothelial cells (**Figure 2G**). This relationship seemed to be causal as the siRNA-mediated knockdown of HuR in CSE-deficient murine endothelial cells decreased CD62E protein expression to basal levels (**Figure 2H**). Taken together, our data indicate that the sulfhydration of HuR by CSE-derived H_2S reduces its ability to bind to its target mRNAs (e.g. CD62E).

Consequences of disturbed flow and vascular inflammation on CSE activity

To study the influence of CSE on the induction of atherosclerosis associated with disturbed flow and low shear stress, $ApoE^{-/-}$ mice were subjected to partial ligation of the left carotid artery.[25] Carotid artery ligation elicited a clear time-dependent (over 3 weeks) increase in CSE expression in CD31 positive cells followed by an increase in vascular smooth muscle cells (**Figure 3A**). Surprisingly this was associated with a decrease rather than an increase in H_2S production (**Figure 3B**). CSE expression was also clearly elevated in atherosclerotic plaques from individuals who had undergone endarterectomy due to 75-85% internal carotid artery stenosis (**Figure 3C&D**). Similar to the situation in mice, circulating (**Figure 3E**) and intra-arterial levels of H_2S (**Figure 3F**) were reduced in human subjects with atherosclerosis.

The decrease in CSE activity was not a consequence of substrate deficiency as levels of the CSE substrate, L-cysteine, were increased in plasma from subjects with atherosclerosis versus healthy donors (**Figure 4A**, **Supplemental Figure 4**, **Supplemental Table 4**). Also, levels of L-cystathionine, which is selectively converted to L-cysteine by CSE, were also markedly increased in plasma from the atherosclerosis group. Circulating levels of the CBS

substrate; L-homocysteine, and its product L-serine, were not significantly different between the two groups.

Next, a link between inflammation and altered CSE activity was addressed. We focused on IL-1β as it was significantly elevated in patients with atherosclerosis compared to healthy donors (**Figure 4B**), and gradually increased during the development of atherosclerosis in mice (**Figure 4C**). In *in vitro* studies, the stimulation of endothelial cells with IL-1β elicited the phosphorylation of CSE on serine as well as on tyrosine, but not threonine residues (**Supplemental Figure 5A-C**). Of the conserved potentially phosphorylatable amino acids the mutation of Tyr60 (human sequence) or Tyr114 (to Phe) partially inhibited CSE activity. The mutation of Ser282 (to either Ala or Asp) was without effect, while the mutation of Ser377 to Asp abrogated CSE activity (**Supplemental Figure 5D&E**). Importantly, while IL-1β attenuated H_2S production in HEK-293 cells transfected with the wild-type CSE, the Ser377Ala CSE mutant was resistant to the cytokine (**Figure 4D**).

Using an antibody that specifically recognized CSE phosphorylated on Ser377, it was possible to demonstrate the serine phosphorylation of a V5-CSE fusion protein immunoprecipitated from IL-1β-treated human endothelial cells, which coincided with a decrease in H_2S production (**Supplemental Figure 5F&G**). The phosphorylation of CSE on Ser377 was also increased in murine carotid arteries one and three weeks after ligation (**Figure 4E**), as well as in human atherosclerotic plaques (**Figure 4F**, **Supplemental Figure 5H**). IL-1β also slightly attenuated the activity of CBS but did not affect that of 3MST (**Supplemental Figure 6A**). The contribution of CBS to endothelial cell H_2S production was however small as IL-1β had only a minor effect (approximately 6% decrease) on H_2S production in endothelial

cells lacking CSE (**Supplemental Figure 6B**). Taken together, these data suggest that vascular inflammation elicits the phosphorylation of CSE and its inactivation.

Consequences of endothelial cell-specific deletion of CSE on atherogenesis

To assess the role of endothelial cell CSE on atherogenesis in a model associated with disturbed flow, endothelial cell specific CSE knockout mice ($CSE^{\Delta EC}$ mice) were crossed onto the $ApoE^{-/-}$ background and subjected to partial ligation of the left carotid artery. Twenty one days after ligation, the lumen area was clearly reduced in arteries from $ApoE^{-/-}$ mice, however, the effects were much more pronounced in carotid arteries from $ApoExCSE^{\Delta EC}$ mice (**Figure 5A**). Micro-CT analyses confirmed the extensive atherosclerotic plaque formation and a decrease in lumen area along the length of the carotid artery in animals lacking endothelial cell CSE (**Figure 5B**). Using a biotin switch-coupled proximity ligation assay, HuR sulfhydration could be demonstrated in carotid artery endothelial cells *in situ* (**Figure 5C&D**). However, this signal rapidly decreased (within 2 days) following partial carotid artery ligation. With disease progression a significant reduction in HuR sulfhydration in vascular smooth muscle cells also became apparent. In line with the decrease in H_2S levels in plasma and tissue from humans with atherosclerosis, the sulfhydration of HuR was also decreased in plaque material compared to healthy arteries (**Figure 5E**). Unfortunately, the CSE target studied in murine endothelial cells i.e., CD62E, was not detected in the available human atherosclerotic plaque material, but a second HuR-regulated protein i.e., cathepsin S (CTSS),[26] was increased in the human plaque versus non-plaque material (**Supplemental Figure 7A**). Indeed, when HuR was immunoprecipitated from CSE overexpressing endothelial cells, its binding to the CTSS 3' untranslated region was decreased (**Supplemental Figure 7B**). Overexpression of the

phosphomimetic Ser377Asp CSE mutant, however, increased the binding of HuR to CTSS mRNA (**Supplemental Figure 7C**).

Effect of the polysulfide donor SG1002 on the development of atherosclerosis

To demonstrate the importance of H_2S in the process of atherogenesis, rescue experiments were performed using sodium polysulthionate (SG1002); a slow releasing polysulfide donor[27,28] that more closely recapitulates the endogenous production of H_2S than fast releasing sulfur salts (**Figure 6A**). In endothelial cells from $CSE^{i\Delta EC}$ mice, the compound was able to restore HuR sulfhydration (**Figure 6B**), as well as to decrease CD62E protein levels (**Figure 6C**) and attenuate monocyte adherence (**Figure 6D**). In mice the addition of SG1002 to the drinking water increased circulating H_2S levels by approximately 60% within 48 hours (**Figure 6E**), a level that remained stable over the observation period. Importantly, plaque formation in $ApoExCSE^{\Delta EC}$ mice 21 days after partial carotid artery ligation was significantly attenuated in the animals that received SG1002 (**Figure 6F&G**). Also, RNA immunoprecipitation studies revealed reduced binding of HuR to CTSS mRNA in ligated arteries from the SG1002-treated mice (**Figure 6H**). There was no direct effect of SG1002 on CSE activity, as plasma levels of its substrates were unaffected (**Supplemental Figure 8A&B**, **Supplemental Table 5**). The effects of SG1002 were also independent of an increase in NOS activity as nitrite levels did not differ compared to the vehicle-treated animals (**Supplemental Figure 8C**). In fact plasma levels of L-arginine increased while levels of L-citrulline decreased, which would be more indicative of NOS inhibition.

L-cystathionine as a biomarker of endothelial cell dysfunction

Given that our data highlighted the importance of CSE activity in maintaining vascular homeostasis, we next addressed the possibility that changes in plasma levels of the CSE substrate

L-cystathionine could be used as a surrogate marker of CSE activity and endothelial cell function. Amino acid profiling of plasma from wild-type, $CSE^{i\Delta EC}$ and globally CSE-deficient mice revealed that more than 80% of the circulating L-cystathionine was seemingly metabolized by endothelial cells (**Figure 7A**). Moreover, the attenuated acetylcholine-induced relaxation of aortic rings from $ApoExCSE^{\Delta EC}$ versus $ApoE^{-/-}$ mice (**Figure 7B**) was coincident with a clear increase in circulating L-cystathionine but a decrease in H_2S levels (**Figure 7C**). A similar reciprocal relationship between L-cystathionine and H_2S levels was also noted between wild-type and $CSE^{i\Delta EC}$ mice.

In a small human cohort, non-invasive recording of vascular reactivity revealed impaired endothelial function (flow-mediated dilatation) in patients with atherosclerosis (**Figure 7D**, **Supplemental Table 6**). In this group, endothelial dysfunction was also linked to increased plasma L-cystathionine levels (**Figure 7E**). In a larger collective the situation was clearer and donors without atherosclerosis could be classified as a L-$cystathionine^{low}/H_2S^{high}$ population while the subjects with atherosclerosis were generally classed as L-$cystathionine^{high}/H_2S^{low}$ (**Figure 7F**). Although, the reciprocal relationship between L-cystathionine, H_2S and the health condition (no plaque versus plaque) was not fully characterized and a prediction model for L-cystathionine levels in the diseased population was not presented, our data indicate that in the pathological conditions in which CSE fails to generate H_2S the levels of its substrate, L-cystathionine, increase in the circulation.

Discussion

The results of the present investigation revealed that CSE is the major source of endogenous H_2S in native endothelial cells and that its expression and activity are tightly regulated by fluid shear

stress and inflammation. The basal activity of CSE was important to maintain low arterial levels of CD62E and minimize monocyte adhesion at sites of low or disturbed flow via a mechanism involving the sulfhydration of the RNA-binding protein, HuR. In inflammatory conditions, however, this protective mechanism was lost because of the phosphorylation (on Ser377) and inactivation of CSE. The loss of H_2S and attenuated sulfhydration of HuR, resulted in an increase in HuR dimerization and activity as well as the stabilization of HuR-target mRNAs e.g. CD62E and CTSS, both of which has previously been linked with endothelial cell activation and atherosclerosis (**Supplemental Figure 9**). Importantly, all of the observations made in a murine model of atherogenesis could be confirmed in a human cohort, making a strong case for a functional link between CSE inactivation and accelerated disease progression. Moreover, at least in mice, a H_2S donor was able to decrease HuR binding to CTSS and decelerate atherogenesis. Finally, in both mice and humans, circulating L-cystathionine levels were inversely correlated with H_2S levels and endothelial function highlighting its potential usefulness as a biomarker of vascular disease.

Ever since the initial report that CSE is expressed in endothelial cells,[6] it has been attributed a major role in generating endothelial cell-derived H_2S.[29] It was possible to confirm this assumption by generating mice lacking CSE specifically in endothelial cells, in which circulating H_2S levels were attenuated by approximately 65%. Moreover, fluid shear stress was found to be a major negative regulator of CSE expression *in situ* and *in vitro*, so that the expression of the enzyme was elevated at sites of low or disturbed blood flow, which are predilection sites for the development of atherosclerosis. It seems that the CSE expressed at these sites exerts a protective function that can at least be partly attributed to repressing the expression of CD62E. However, as CSE-derived H_2S did not directly target CD62E an indirect approach

was taken to identify potential sulfhydration targets that could in turn account for the effects observed. Reasoning that CSE should associate with H_2S targets, co-precipitation studies identified the RNA binding protein, HuR, as part of the CSE interactome. HuR was an attractive candidate for sulfhydration as it possesses three cysteines, one of which is predicted to be highly nucleophilic. Indeed, it was possible to detect the sulfhydration of HuR in wild-type endothelial cells, which was barely detectable in cells lacking CSE. The finding that Cys13 was targeted by H_2S, hinted at a possible molecular mechanism as Cys13 is essential for the formation of the disulfide bonds that stabilize the active HuR homodimer.[24] The sulfhydration of HuR in CSE-expressing endothelial cells meant that HuR was detected largely as an inactive monomer that was unable to bind its target mRNA i.e. CD62E.

To evaluate the pathophysiological relevance of these findings, the expression and activity of CSE was studied in a murine model of atherogenesis linked with disturbed flow.[25] Consistent with the *in vitro* observations, CSE was significantly up-regulated one week after partial carotid artery ligation. More importantly, in samples from patients with carotid artery stenosis (75-85%) that demonstrated disturbed or low flow, CSE levels were clearly upregulated. Somewhat unexpectedly, however, the clear increase in arterial CSE expression, contrasted with the marked reduction in circulating and tissue levels of H_2S, indicating that endothelial dysfunction and atherosclerosis were linked to the inhibition of CSE activity. In agreement with this observation, partial ligation of the carotid artery in mice led to a time-dependent decrease in the sulfhydration of HuR. The latter effects could not be attributed to CSE inactivity due to substrate deficiency as the amino acid profile of human plasma and plaque material revealed that levels of the CSE-specific substrate L-cystathionine were actually elevated. Given the link between vascular inflammation and atherosclerosis, the consequences of inflammatory cytokines

on CSE activity were assessed. IL-1β was chosen for these studies because its levels were increased in the mouse model as well as in the available human samples. Indeed, IL-1β elicited the serine phosphorylation of CSE and, in agreement with a previous report[30], it was possible to demonstrate that the serine phosphorylation of CSE on Ser377 resulted in enzyme inactivation. Making the link back to atherosclerosis, the serine phosphorylation of CSE was detectable in carotid arteries from the murine model of atherosclerosis as well as in plaque material from individuals with atherosclerosis. The inactivation of CSE in humans could be linked to decreased sulfhydration of HuR and increased expression of the HuR target CTSS. There are, of course a number of additional, recently identified targets of H_2S donors that could contribute to the phenotype observed, including sirtuin-1[31], which is also stabilized by HuR[20,32]. A number of additional proteins physically associated with CSE in endothelial cells including collagen and two pacsin proteins that are implicated in vesicle trafficking,[33,34] and it will be interesting to determine whether the sulfhydration of these proteins can also affect vascular homeostasis. Animal models of atherosclerosis are generally based on plaque formation due to a cholesterol-rich/Western-type diet, in combination with the manipulation of genes involved in cholesterol metabolism. Although these mouse models have provided a wealth of insight into disease pathogenesis, each of them comes with its own limitations.[35] The $ApoE^{-/-}$ model studied here was chosen because of the initial link to disturbed flow and the accelerated development of atherosclerotic lesions. Given the potential limitations of this model we placed a particular emphasis on comparing changes observed in the animal model with samples from humans with and without atherosclerosis. By taking this dual approach it was possible to confirm the altered sulfhydration of HuR, upregulation of CSE expression in atherosclerotic plaques, the

phosphorylation of CSE, a subsequent decrease in H_2S levels, as well as alterations in the amino acid profile that correlated with CSE activity in human material.

To determine the importance of endothelial cell CSE in atherogenesis studies were repeated in mice specifically lacking CSE in endothelial cells. Consistent with a key role of the endothelium in atherosclerosis initiation, plaque size was greater and carotid lumen size smaller in partially ligated carotid arteries from ApoExCSE$^{\Delta EC}$ mice versus ApoE$^{-/-}$ mice. Thus, although H_2S has been proposed to freely diffuse across membranes,[3] it seems that the H_2S produced in smooth muscle cells cannot substitute for the loss of endothelial cell-derived H_2S. Given the apparent important anti-atherosclerotic role of CSE, the next step was to assess the consequences of exogenous H_2S application on the development of atherosclerosis. The rescue proved to be efficient *in vitro* as the H_2S donor SG1002 largely restored the sulfhydration of HuR and decreased the expression of CD62E as well as monocyte adhesion in CSE-deficient endothelial cells. Moreover, the *in vivo* administration of SG1002 to ApoExCSE$^{\Delta EC}$ mice resulted in a maintained elevation in plasma H_2S levels and a pronounced reduction in atherosclerosis. Preclinical studies have demonstrated that SG1002 is also able to attenuate cardiac dysfunction, protect against pressure overload-induced heart failure (reviewed in reference[27]) and to restore plasma H_2S and NO levels to normal in patients with congestive heart failure[36]. However, there was no indication of elevated NO production in our studies as assessed by amino acid profiling and assay of circulating nitrite levels, thus suggesting that the anti-atherosclerotic actions of SG1002 can be attributed directly to H_2S.

The amino acid profiling studies also suggested that high plasma levels of L-cystathionine mirrored decreased CSE activity. Therefore, in a final step, we set out to determine whether or not circulating levels of L-cystathionine could be used as a biomarker of endothelial

dysfunction. By comparing plasma from the available wild-type, globally CSE-deficient and endothelial cell-specific CSE knockout mice, it was possible to demonstrate that altering endothelial cell CSE activity had a major impact on circulating L-cystathionine levels. Importantly, high plasma L-cystathionine levels also correlated with impaired endothelial function in ApoExCSE$^{\Delta EC}$ versus ApoE$^{-/-}$ mice. Similarly, circulating L-cystathionine levels were negatively correlated with H_2S production in patients with atherosclerosis compared to healthy subjects. Moreover, in a small cohort of subjects it was possible to classify those patients with atherosclerosis and attenuated flow-induced vasodilatation as being L-cystathionine^{high}/H_2S^{low}. All of these data indicate that plasma levels of L-cystathionine and/or H_2S could be useful biomarkers of endothelial dysfunction in non diagnosed asymptomatic individuals with early vascular disease.

Taken together, the results of this study have highlighted the importance of CSE in endothelial cells for the prevention of atherosclerosis development, identified HuR as a primary molecular target of endogenous H_2S that can account for pro-atherosclerotic changes in the vessel wall following CSE inactivation, and provided evidence that L-cystathionine is an effective biomarker of impaired endothelial dysfunction.

Authors

Sofia-Iris Bibli, PhD[1,2]; Jiong Hu, PhD[1,2]; Fragiska Sigala, MD[3]; Ilka Wittig, PhD[2,4]; Juliana Heidler, PhD[2,4]; Sven Zukunft, PhD[1,2]; Diamantis I. Tsilimigras, MD[3]; Voahanginirina Randriamboavonjy, PhD[1,2]; Janina Wittig, BSc[1,2]; Baktybek Kojonazarov, PhD[5]; Christoph Schürmann, PhD[2,6]; Mauro Siragusa, PhD[1,2]; Daniel Siuda, PhD[1,2]; Bert Luck, MSc[1,2]; Randa Abdel Malik, PhD[1,2]; Konstantinos A. Filis, MD[3]; George Zografos, MD[3];

Chen Chen, MD[7]; Dao Wen Wang, MD[7]; Josef Pfeilschifter, MD[8]; Ralf P. Brandes, MD[2,6]; Csaba Szabo, PhD[9]; Andreas Papapetropoulos, PhD[10]; Ingrid Fleming, PhD[1,2]

Affiliations

[1]Institute for Vascular Signalling, Centre for Molecular Medicine, Goethe University, Frankfurt am Main, Germany; [2]German Center of Cardiovascular Research (DZHK), Partner site RheinMain, Frankfurt am Main, Germany; [3]First Propedeutic Department of Surgery, Vascular Surgery Division, National and Kapodistrian University of Athens Medical School, Athens, Greece; [4]Functional Proteomics, SFB 815 Core Unit, Goethe University, Frankfurt am Main, Germany; [5]Department of Internal Medicine, Universities of Giessen and Marburg Lung Center, Justus Liebig University, Giessen, Germany; [6]Institute for Cardiovascular Physiology, Goethe University, Frankfurt am Main, Germany; [7]Division of Cardiology, Department of Internal Medicine and Gene Therapy Center, Tongji Hospital, Tongji Medical College, Huazhong University of Science and Technology, Wuhan, China; [8]Pharmacentre Frankfurt/ZAFES, Goethe University, Frankfurt am Main, Germany; [9]Laboratory of Pharmacology, Department of Medicine, University of Fribourg, Fribourg, Switzerland; [10]Clinical, Experimental Surgery and Translational Research Center, Biomedical Research Foundation of the Academy of Athens, Athens, Greece

Acknowledgments

The authors are indebted to Isabel Winter, Mechtild Piepenbrock-Gyamfi and Katharina Herbig for expert technical assistance and to Mr. Andersen Clark from University Medical Texas Medical Branch for help with statistical analyses.

Sources of Funding

This work was supported by the European Society of Cardiology (Basic Research Fellowship 2016 and Research Grant R-2016-054), the Schering Stiftung (Young Investigator Fund for Innovative Research 2017, to S.-I.B) and the Deutsche Forschungsgemeinschaft (SFB 815/A6 to I.F., SFB 815/A7 to J.P. and Exzellenzcluster 147 "Cardio-Pulmonary Systems").

Author Contributions

S-I.B., J.Hu. and I.F. designed and guided research; S-I.B., J.Hu, J.H., V.R., D.T., J.W., and R.A.M. performed experiments; S-I.B., J.Hu. and I.F. analyzed data. I.W. and J.H, performed the proteomic analyses; S.Z. performed the amino acid profiling and analysis; D.S. performed amino acid analyses; B.K. performed the echocardiography; M.S. measured the circulating nitrite levels; B.L. and S.Z. analyzed H_2S levels; C.C. and D.W.W. provided immunohistochemistry stainings in human material; J.P. generated the floxed CSE mouse; C.Z. raised the phospho-specific Ser377 CSE specific antibody; F.S. and D.T. provided human samples and performed the vascular function studies in humans; F.S., KA.F. and G.Z. analyzed the human vascular function studies and provided the echochardiography human data; A.P. provided viruses, mutants and activity data for H_2S generating enzymes. C.S. and R.P.B. performed the µCT analyses; F.S., C.S., and A.P provided conceptual advice; S.-I.B. and I.F. wrote the manuscript.

Competing Financial Interests

The authors declare no competing financial interests

Conflict of Interest Disclosures

Sofia-Iris Bibli: None

Jiong Hu: None

Fragiska Sigala: None

Ilka Wittig: None

Juliana Heidler: None

Sven Zukunft: None

Diamantis I. Tsilimigras: None

Voahanginirina Randriamboavonjy: None

Janina Wittig: None

Baktybek Kojonazarov: None

Christoph Schürmann: None

Mauro Siragusa: None

Daniel Siuda: None

Bert Luck: None

Randa Abdel Malik: None

Konstantinos A. Filis: None

George Zografos: None

Chen Chen: None

Dao Wen Wang:

Josef Pfeilschifter: None

Ralf P. Brandes: None

Csaba Szabo: None

Andreas Papapetropoulos: None

Ingrid Fleming: None

References

1 Ross R, Glomset JA. Atherosclerosis and the arterial smooth muscle cell. *Science*. 1973;180:1332. doi: 10.1126/science.180.4093.1332

2 Davies PF, Civelek M, Fang Y, Fleming I. The atherosusceptible endothelium: endothelial phenotypes in complex hemodynamic shear stress regions *in vivo*. *Cardiovasc Res*. 2013;99:315-327. doi: 10.1093/cvr/cvt101

3 Wang R. Physiological implications of hydrogen sulfide: a whiff exploration that blossomed. *Physiol Rev*. 2012;92:791-896. doi: 10.1152/physrev.00017.2011

4 Shibuya N, Koike S, Tanaka M, Ishigami-Yuasa M, Kimura Y, Ogasawara Y, Fukui K, Nagahara N, Kimura H. A novel pathway for the production of hydrogen sulfide from D-cysteine in mammalian cells. *Nat Commun*. 2013;4:1366. doi: 10.1038/ncomms2371

5 Szabo C, Papapetropoulos A. International Union of Basic and Clinical Pharmacology. CII: Pharmacological modulation of H_2S levels: H_2S donors and H_2S biosynthesis inhibitors. *Pharmacol Rev*. 2017;69:497-564

6 Yang G, Wu L, Jiang B, Yang W, Qi J, Cao K, Meng Q, Mustafa AK, Mu W, Zhang S, Snyder SH, Wang R. H_2S as a physiologic vasorelaxant: hypertension in mice with deletion of cystathionine g-lyase. *Science*. 2008;322:587. doi: 10.1126/science.1162667

7 Syhr KMJ, Boosen M, Hohmann SW, Longen S, Köhler Y, Pfeilschifter J, Beck KF, Geisslinger G, Schmidtko A, Kallenborn-Gerhardt W. The H_2S-producing enzyme CSE is dispensable for the processing of inflammatory and neuropathic pain. *Brain Res*. 2015;1624:380-389. doi: 10.1016/j.brainres.2015.07.058

8 Mani S, Li H, Untereiner A, Wu L, Yang G, Austin RC, Dickhout JG, Lhoták S, Meng QH, Wang R. Decreased endogenous production of hydrogen sulfide accelerates atherosclerosis. *Circulation*. 2013;127:2523. doi: 10.1161/CIRCULATIONAHA.113.002208

9 Li H, Mani S, Cao W, Yang G, Lai C, Wu L, Wang R. Interaction of hydrogen sulfide and estrogen on the proliferation of vascular smooth muscle cells. *PLoS ONE*. 2012;7:e41614. doi:10.1371/journal.pone.0041614

10 Li H, Mani S, Wu L, Fu M, Shuang T, Xu C, Wang R. The interaction of estrogen and CSE/H_2S pathway in the development of atherosclerosis. *Am J Physiol Heart Circ Physiol*. 2016;312:H406-H414. doi: 10.1152/ajpheart.00245.2016

11 Cheung SH, Kwok WK, To KF, Lau JYW. Anti-atherogenic effect of hydrogen sulfide by over-expression of cystathionine gamma-lyase (CSE) gene. *PLoS ONE*. 2014;9:e113038. doi: 10.1371/journal.pone.0113038

12 van den Born JC, Mencke R, Conroy S, Zeebregts CJ, van Goor H, Hillebrands JL. Cystathionine g-lyase is expressed in human atherosclerotic plaque microvessels and is involved in micro-angiogenesis. *Sci Rep*. 2016;6:34608. doi: 10.1038/srep34608

13 Sigala F, Efentakis P, Karageorgiadi D, Filis K, Zampas P, Iliodromitis EK, Zografos G, Papapetropoulos A, Andreadou I. Reciprocal regulation of eNOS, H_2S and CO-synthesizing enzymes in human atheroma: correlation with plaque stability and effects of simvastatin. *Redox Biol*. 2017;12:70-81. doi: 10.1016/j.redox.2017.02.006

14 Yu B, Zheng Y, Yuan Z, Li S, Zhu H, De La Cruz LK, Zhang J, Ji K, Wang S, Wang B. Toward direct protein S-persulfidation: a prodrug approach that directly delivers hydrogen persulfide. *J Am Chem Soc*. 2018;140:30-33. doi: 10.1021/jacs.7b09795

15 Paul BD, Snyder SH. Protein sulfhydration. *Methods Enzymol*. 2015;555:79-90. doi: 10.1016/bs.mie.2014.11.021

16 Monvoisin A, Alva JA, Hofmann JJ, Zovein AC, Lane TF, Iruela-Arispe ML. VE-cadherin-CreERT2 transgenic mouse: a model for inducible recombination in the endothelium. *Dev Dyn*. 2006;235:3413-3422. doi: 10.1002/dvdy.20982
17 Xia J, Sinelnikov IV, Han B, Wishart DS. MetaboAnalyst 3.0-making metabolomics more meaningful. *Nucleic Acids Res*. 2015;43:W251-W257. doi: 10.1093/nar/gkv380
18 Ziegler T, Silacci P, Harrison VJ, Hayoz D. Nitric oxide synthase expression in endothelial cells exposed to mechanical forces. *Hypertension*. 1998;32:351-355. doi: 10.1161/01.HYP.32.2.351
19 Ziegler T, Bouzourene K, Harrison VJ, Brunner HR, Hayoz D. Influence of oscillatory and unidirectional flow environments on the expression of endothelin and nitric oxide synthase in cultured endothelial cells. *Arterioscler Thromb Vasc Biol*. 1998;18:686-692. doi: 10.1161/01.ATV.18.5.686
20 Ceolotto G, De Kreutzenberg SV, Cattelan A, Fabricio ASC, Squarcina E, Gion M, Semplicini A, Fadini GP, Avogaro A. Sirtuin 1 stabilization by HuR represses TNF-a- and glucose-induced E-selectin release and endothelial cell adhesiveness *in vitro*: relevance to human metabolic syndrome. *Clin Sci*. 2014;127:449. doi: 10.1042/CS20130439
21 Olsson MH, Sondergaard CR, Rostkowski M, Jensen JH. PROPKA3: consistent treatment of internal and surface residues in empirical pKa predictions. *J Chem Theory Comput*. 2011;7:525-537. doi: 10.1021/ct100578z
22 Ferre F, Clote P. DiANNA: a web server for disulfide connectivity prediction. *Nucleic Acids Res*. 2005;33:W230-W232. doi: 10.1093/nar/gki412
23 Ferre F, Clote P. DiANNA 1.1: an extension of the DiANNA web server for ternary cysteine classification. *Nucleic Acids Res*. 2006;34:W182-W185. doi: 10.1093/nar/gkl189
24 Benoit RM, Meisner NC, Kallen J, Graff P, Hemmig R, Cèbe R, Ostermeier C, Widmer H, Auer M. The X-ray crystal structure of the first RNA recognition motif and site-directed mutagenesis suggest a possible HuR redox sensing mechanism. *J Mol Biol*. 2010;397:1231-1244. doi: 10.1016/j.jmb.2010.02.043
25 Nam D, Ni CW, Rezvan A, Suo J, Budzyn K, Llanos A, Harrison D, Giddens D, Jo H. Partial carotid ligation is a model of acutely induced disturbed flow, leading to rapid endothelial dysfunction and atherosclerosis. *Am J Physiol - Heart Circ Physiol*. 2009;297:H1535-H1543. doi: 10.1152/ajpheart.00510.2009
26 Stellos K, Gatsiou A, Stamatelopoulos K, Perisic Matic L, John D, Lunella FF, Jae N, Rossbach O, Amrhein C, Sigala F, Boon RA, Furtig B, Manavski Y, You X, Uchida S, Keller T, Boeckel JN, Franco-Cereceda A, Maegdefessel L, Chen W, Schwalbe H, Bindereif A, Eriksson P, Hedin U, Zeiher AM, Dimmeler S. Adenosine-to-inosine RNA editing controls cathepsin S expression in atherosclerosis by enabling HuR-mediated post-transcriptional regulation. *Nat Med*. 2016;22:1140-1150. doi: 10.1038/nm.4172
27 Wallace JL, Vaughan D, Dicay M, MacNaughton WK, de Nucci G. Hydrogen sulfide-releasing therapeutics: translation to the clinic. *Antioxid Redox Signal*. 2017;28:1533-1540. doi: 10.1089/ars.2017.7068
28 Chappell DC, Varner SE, Nerem RM, Medford RM, Alexander RW. Oscillatory shear stress stimulates adhesion molecule expression in cultured human endothelium. *Circ Res*. 1998;82:532. doi: 10.1161/01.RES.82.5.532
29 Polhemus DJ, Lefer DJ. Emergence of hydrogen sulfide as an endogenous gaseous signaling molecule in cardiovascular disease. *Circ Res*. 2014;114:730. doi: 10.1161/CIRCRESAHA.114.300505

30 Yuan G, Vasavda C, Peng YJ, Makarenko VV, Raghuraman G, Nanduri J, Gadalla MM, Semenza GL, Kumar GK, Snyder SH, Prabhakar NR. Protein kinase G-regulated production of H_2S governs oxygen sensing. *Sci Signal*. 2015;8:ra37. doi: 10.1126/scisignal.2005846
31 Du C, Lin X, Xu W, Zheng F, Cai J, Yang J, Cui Q, Tang C, Cai J, Xu G, Geng B. Sulfhydrated sirtuin-1 increasing its deacetylation activity is an essential epigenetics mechanism of anti-atherogenesis by hydrogen sulfide. *Antioxid Redox Signal*. 2018; doi:10.1089/ars.2017.7195.
32 Abdelmohsen K, Pullmann R, Lal A, Kim HH, Galban S, Yang X, Blethrow JD, Walker M, Shubert J, Gillespie DA, Furneaux H, Gorospe M. Phosphorylation of HuR by Chk2 regulates SIRT1 expression. *Mol Cell*. 2007;25:543-557. doi: 10.1016/j.molcel.2007.01.011
33 Kessels MM, Qualmann B. The syndapin protein family: linking membrane trafficking with the cytoskeleton. *J Cell Sci*. 2004;117:3077. doi: 10.1242/jcs.01290
34 Dorland YL, Malinova TS, van Stalborch AM, Grieve AG, van Geemen D, Jansen NS, de Kreuk BJ, Nawaz K, Kole J, Geerts D, Musters RJP, de Rooij J, Hordijk PL, Huveneers S. The F-BAR protein pacsin2 inhibits asymmetric VE-cadherin internalization from tensile adherens junctions. *Nat Commun*. 2016;7:12210. doi: 10.1038/ncomms12210
35 Emini Veseli B, Perrotta P, De Meyer GRA, Roth L, Van der Donckt C, Martinet W, De Meyer GRY. Animal models of atherosclerosis. *Eur J Pharmacol*. 2017;816:3-13. doi: 10.1016/j.ejphar.2017.05.010
36 Polhemus DJ, Li Z, Pattillo CB, Gojon G, Gojon G, Giordano T, Krum H. A novel hydrogen sulfide prodrug, SG1002, promotes hydrogen sulfide and nitric oxide bioavailability in heart failure patients. *Cardiovasc Ther*. 2015;33:216-226. doi: 10.1111/1755-5922.12128

Figure Legends

Figure 1. CSE regulation and effects in endothelial cells. A| *En face* staining showing the expression of CSE (red) and CD144 (green) in different areas of aorta. 1: lesser curvature, 2: subclavian artery, 3: carotid artery, 4: descending aorta, 5: thoracic artery branch point. Samples from $CSE^{i\Delta EC}$ mice were included as a negative control. DAPI (grey), bar = 5µm. **B**| Quantification of CSE expression, n=6 mice per group (ANOVA, Newman-Keuls). **C**| Time course of the changes in CSE and eNOS protein expression in human endothelial cells exposed to fluid shear stress (12 dynes/cm^2) for up to 48 hours. CSE-expressing HEK-293 cells were included as a positive control (PC). **D**| Time course of the changes in CSE and eNOS protein expression (quantification of data in panel B) and H_2S production in human endothelial cells exposed to fluid shear stress (12 dynes/cm^2) for up to 48 hours. All values are relative to levels in cells maintained under static conditions, n=6-12 experiments using 5-7 different cell batches (2 way ANOVA, Bonferonni, versus static/0h). **E**| Expression of CSE and CD62E in cultured endothelial cells from wild-type (WT) and $CSE^{i\Delta EC}$ (iΔEC) mice treated with solvent or IL-1β (30 ng/ml) for 3 hours. The graphs summarize n=6-9 experiments from 6 different batches of endothelial cells (ANOVA, Newman-Keuls). **P<0.01, ***P<0.001

Figure 2. Link between CSE-derived H_2S and the sulfhydration of HuR on Cys13. A| Co-precipitation of HuR with CSE from murine endothelial cells transduced with GFP or CSE adenoviruses; IP = immunoprecipitation. Results are representative of a further 4 cell batches. **B**| Sulfhydrated HuR (S-SH) and total HuR in endothelial cells from wild-type and $CSE^{i\Delta EC}$ mice. DTT was included to demonstrate specificity by quenching the signal. Comparable results were obtained in an additional 5 experiments (Student's t test). **C**| HuR sulfhydration (HuR-S-SH; red)

in endothelial cells from wild-type (WT) and $CSE^{i\Delta EC}$ (iΔEC) mice detected using a biotin switch-coupled proximity ligation assay. Blue = phalloidin, cyan = DAPI, non biotinylated WT cells were used as negative control. Similar results were observed using 3 additional batches of cells, bar=10 μm. **D**| Sulfhydration (S-SH) of HuR in HEK-293 cells expressing the wild-type HuR or the different cysteine mutants. Similar results were obtained in 3 additional experiments. **E**| HuR monomers (m) and dimers (d) in HEK-293 cells expressing the wild-type HuR or the different cysteine mutants. The blots are representative of a further 4-5 experiments. **F**| HuR monomers (m) and dimers (d) in endothelial cells from wild-type and $CSE^{i\Delta EC}$ mice. Representative blot from n=6 different cell batches. **G**| *CD62E* RNA immunoprecipitated with HuR from endothelial cells from wild-type and $CSE^{i\Delta EC}$ mice, n=6 experiments using 4 different cell batches (Student's t test). The blots demonstrate the equivalent immunoprecipitation (IP) of HuR, and are representative of 3 additional experiments. Sup = supernatant after IP. **H**| Expression of CD62E in endothelial cells from wild-type (WT) and $CSE^{i\Delta EC}$ (iΔEC) mice treated with a control siRNA (siCTL) or siRNA directed against HuR (siHuR). n=6 experiments using 4 different cell batches (2 way ANOVA, Bonferroni). ***P<0.001.

Figure 3. CSE expression in the vascular wall. A| Expression of CSE (red), CD31 (green) and α smooth muscle actin (αSMA, blue) in a non-ligated (NL) carotid artery from an $ApoE^{-/-}$ mouse versus samples collected 2 days, 1 or 3 weeks after partial carotid artery ligation. The white boxes mark the area magnified in the right hand panels. Bar = 20 μm. **B**| Time course of the changes in CSE expression, blood flow and plasma H_2S levels in the same samples as in panel A, n=4 per group (each sample representing a pool of 3 animals) for protein and H_2S levels, and n=6-8 animals per group for blood flow (2 way ANOVA, Bonferonni). **C**| Comparison of CSE

and eNOS expression in plaque free (NP, n=5) arteries and carotid plaques (n=20) from human subjects. **D**| Representative staining of CSE (red), von Willebrand factor (vWF, green), α smooth muscle actin (αSMA, blue) and DAPI (grey) in aortae without atherosclerotic plaque versus carotid atherosclerotic plaques. Similar results were observed in 5 additional subjects per group. Bar = 50 μm **E**|. Plasma H_2S levels in samples from plaque free individuals (NP, n=32) or subjects with atherosclerosis (Plaque, n=70) (Mann Whitney). **F**|. Arterial H_2S levels in arterial tissue from plaque free individuals (NP, n=5) or subjects with atherosclerosis (Plaque, n=20) (Mann Whitney). **P<0.01, ***P<0.001.

Figure 4. Consequences of inflammation on CSE activity in later stages of atherosclerosis. **A**| Circulating levels of L-cysteine, L-cystathionine, L-homocysteine and L-serine in plasma from n=26-32 plaque-free (NP) donors and n=64-70 patients with atherosclerosis (Plaque) (Mann Whitney). **B**| Circulating levels of IL-1β in samples from 12 subjects without (NP) and 30 subjects with plaques (Mann Whitney). **C**| Circulating levels of IL-1β in samples from $ApoE^{-/-}$ mice 2 days (2d), 1 or 3 weeks (1w, 3w) after partial carotid artery ligation, n=4 samples per time point (each sample representing a pool of 3 animals; ANOVA, Newman-Keuls). **D**| H_2S production detected in HEK-293 cells expressing the wild-type (WT) CSE or the S377A and S377D CSE mutants and treated with either solvent or IL-1β (30 ng/ml, 18 hours), n=6 independent experiments (ANOVA, Newman-Keuls). **E**| CSE phosphorylation on Ser377 in non-ligated (NL) or ligated carotid arteries 2 days, 1 and 3 weeks after operation. The graph summarizes data from 4 independent experiments, with each experiment being a pool of 3 animals (ANOVA, Newman-Keuls). **F**| Serine phosphorylation of CSE in human arteries detected by proximity ligation assay (red) using phospho-serine and CSE antibodies. Cyan =

DAPI. Right panels show bright field images merged with DAPI. Similar results were observed in 5 additional subjects per group. bar = 50 µm. ***P<0.001.

Figure 5. Characterization of atherosclerosis development in endothelial cell-specific CSE knockout mice. A-B| Effect of partial ligation on carotid arteries from ApoE$^{-/-}$ and ApoExCSE$^{\Delta EC}$ (ΔEC) mice. (**A**) Representative cross sections showing Oil Red O staining in non-ligated and partially ligated murine carotid arteries. (**B**) Carotid artery lumen evaluated by µCT scanning (ligated arteries in blue) and quantification of lumen area, n=7-8 animals per group; bar = 200 µm (ANOVA for repeated measurements). **C**| HuR sulfhydration (S-SH) and total HuR levels in carotid arteries from ApoE$^{-/-}$ mice with no ligation (NL) and 2 days, 1 week or 3 weeks after partial carotid artery ligation. The results are representative of 4 additional samples (each sample representing a pool of 3 animals) per group. **D**| Sulfhydrated HuR (S-SH; red), CD31 (green) and DAPI (blue) in cross sections from carotid arteries from ApoE$^{-/-}$ mice with no ligation and 2 days or 1 week after partial ligation. DAPI = cyan, bar = 20 µm. Graphs summarize sulfhydration events per endothelial cell (EC) or smooth muscle cell (SMC), n = 6 animals per group (ANOVA, Newman-Keuls). **E**| Sulfhydration of HuR (S-SH) in non-plaque (NP) material as well as in atherosclerotic plaques (Plaque) from human subjects. The results are representative of n=4 NP and n=12 Plaque samples per group. **P<0.01, ***P<0.001.

Figure 6. Effect of SG1002 on the phenotype of ApoExCSE$^{\Delta EC}$ mice. A| H_2S release from murine endothelial cells treated with solvent (Sol), NaHS (100 µmol/L) or SG1002 (SG, 1 µmol/L), n=4 independent cell batches (2 way ANOVA, Bonferroni). **B**| HuR sulfhydration (S-SH) in endothelial cells from wild-type (WT) and CSE$^{i\Delta EC}$ (iΔEC) mice treated with solvent or

SG1002. Results are representative of an additional 4 cell batches. **C**| CD62E levels in endothelial cells from $CSE^{i\Delta EC}$ mice treated with solvent or SG1002 for 60 minutes. Results are representative of an additional 5 cell batches per group. **D**| Monocyte adherence to endothelial cells from wild-type (WT) and $CSE^{i\Delta EC}$ (iEC) mice treated with solvent or SG1002 for 60 minutes. Adherence on fibronectin (F) was included as a negative control and IL-1β (IL, 30 ng/ml, 3 hours) as a positive control, n=12 experiments from 6 different cell batches (ANOVA, Newman-Keuls). **E**| H_2S levels in plasma from $ApoE^{-/-}$ mice given SG1002 (400-600 ng/day) in drinking water, n=6 animals per group (ANOVA, Newman-Keuls). **F-G**| Effect of SG1002 on the development of atherosclerosis. Representative images of Oil Red O staining of left carotid arteries from $ApoExCSE^{\Delta EC}$ mice 21 days after partial ligation. Mice were treated with vehicle (Veh) or SG1002 starting one day prior to partial ligation (F). Carotid artery lumen evaluated by µCT scanning (blue = ligated and red = non-ligated) and quantification of lumen area 21 days after carotid artery ligation in $ApoExCSE^{\Delta EC}$ mice treated with vehicle or SG1002, n=7-8 animals per group (ANOVA for repeated measurements, Dunns) (G). **H**| RNA immunoprecipitation showing the association of the CTSS 3'UTR with HuR in carotid arteries from the animals shown in panels f-g; n=5 per group (Student's t test). **P*<0.05, ***P*<0.01, ****P*<0.001.

Figure 7. L-Cystathionine as a biomarker of CSE activity and endothelial cell dysfunction in humans. A| L-Cystathionine levels in plasma from wild-type (WT), $CSE^{i\Delta EC}$ (iΔEC) and CSE^{iKO} (iKO) mice, n=6-12 animals per group (ANOVA, Newman-Keuls). **B**| Acetylcholine (ACh)-induced relaxation in aortic rings from $ApoE^{-/-}$ and $ApoExCSE^{\Delta EC}$ mice fed a high fat diet for 21 days; n=8 animals per group (2 way ANOVA, Bonferroni). **C**| Linear correlation of

circulating L-cystathionine and H_2S levels in WT, $CSE^{i\Delta EC}$, $ApoE^{-/-}$ and $ApoExCSE^{\Delta EC}$ mice, n=6 animals per group (Pearson). **D**| Flow-mediated dilatation (FMD) and flow-mediated constriction (FMC) in healthy volunteers (n=6) and patients (n=6) with atherosclerotic plaques. **E**| Linear correlation of FMD and circulating L-cystathionine levels in healthy subjects (n=6) without atherosclerosis (NP) and patients (n=6) with atherosclerosis and carotid stenosis between 75-90% (Pearson). **F**| Linear correlation of circulating L-cystathionine and H_2S levels in samples from human subjects without plaques (NP, n=32) and with atherosclerosis (Plaque; n=70) (Pearson). **P<0.01, ***P<0.001

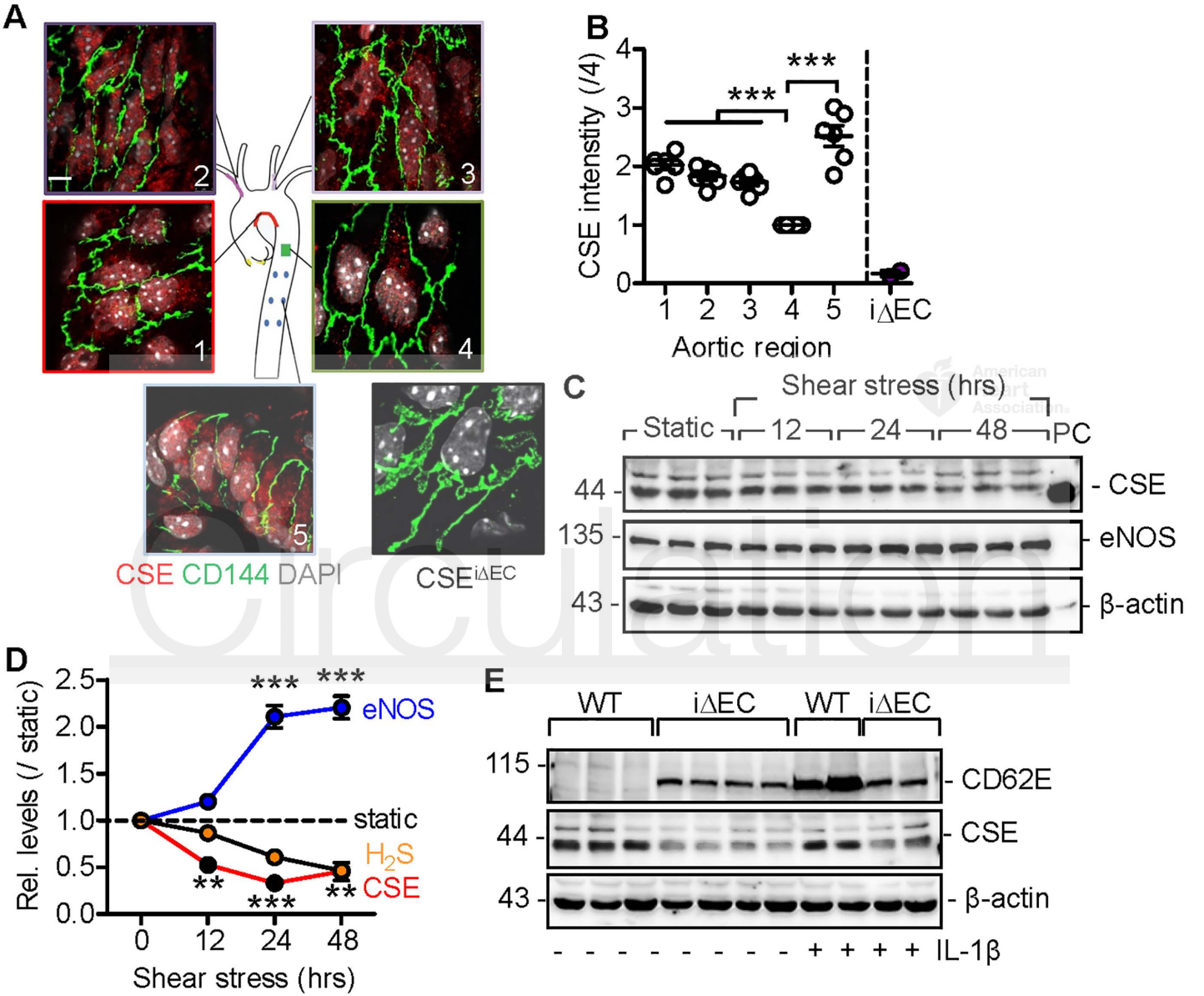

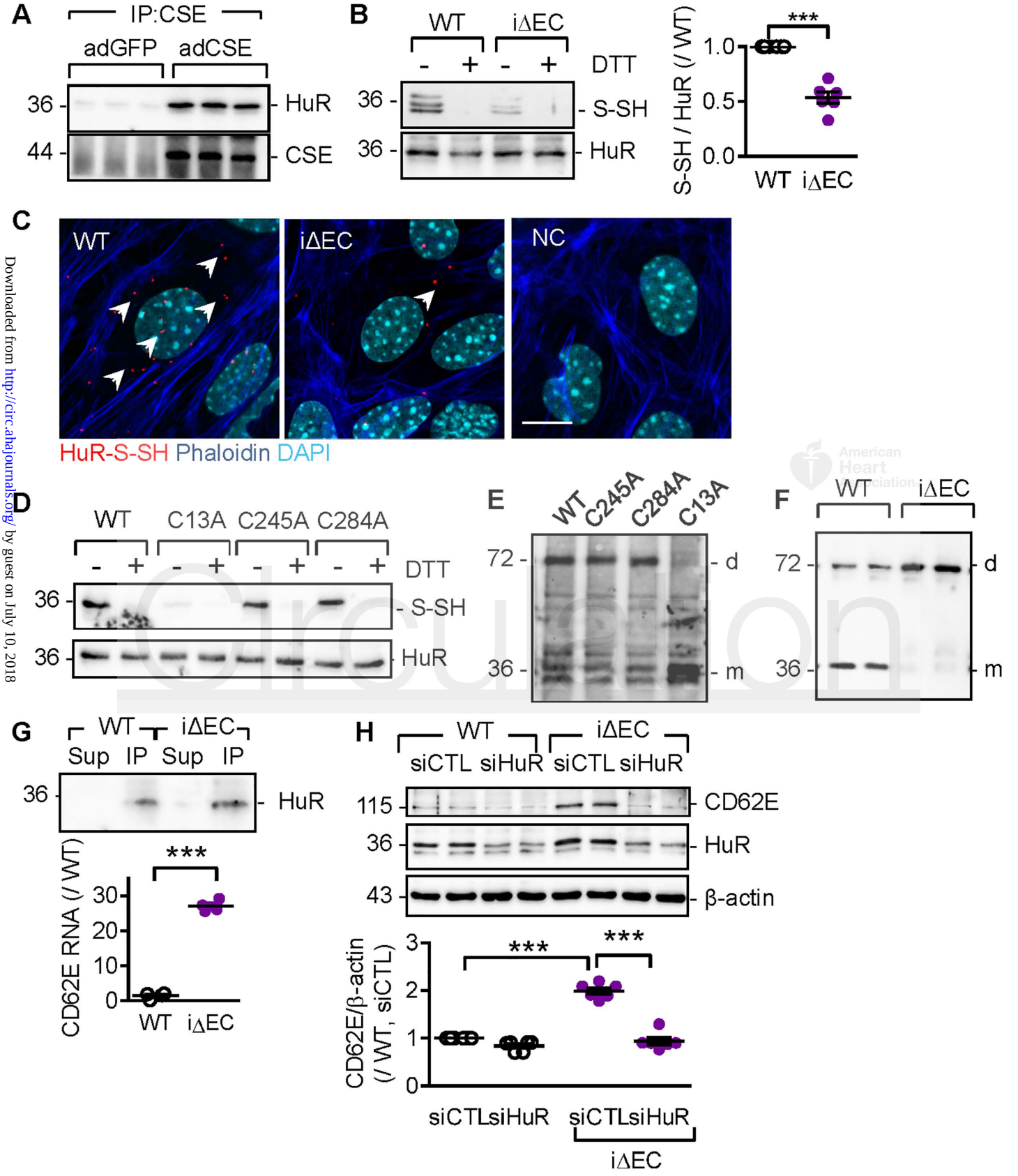

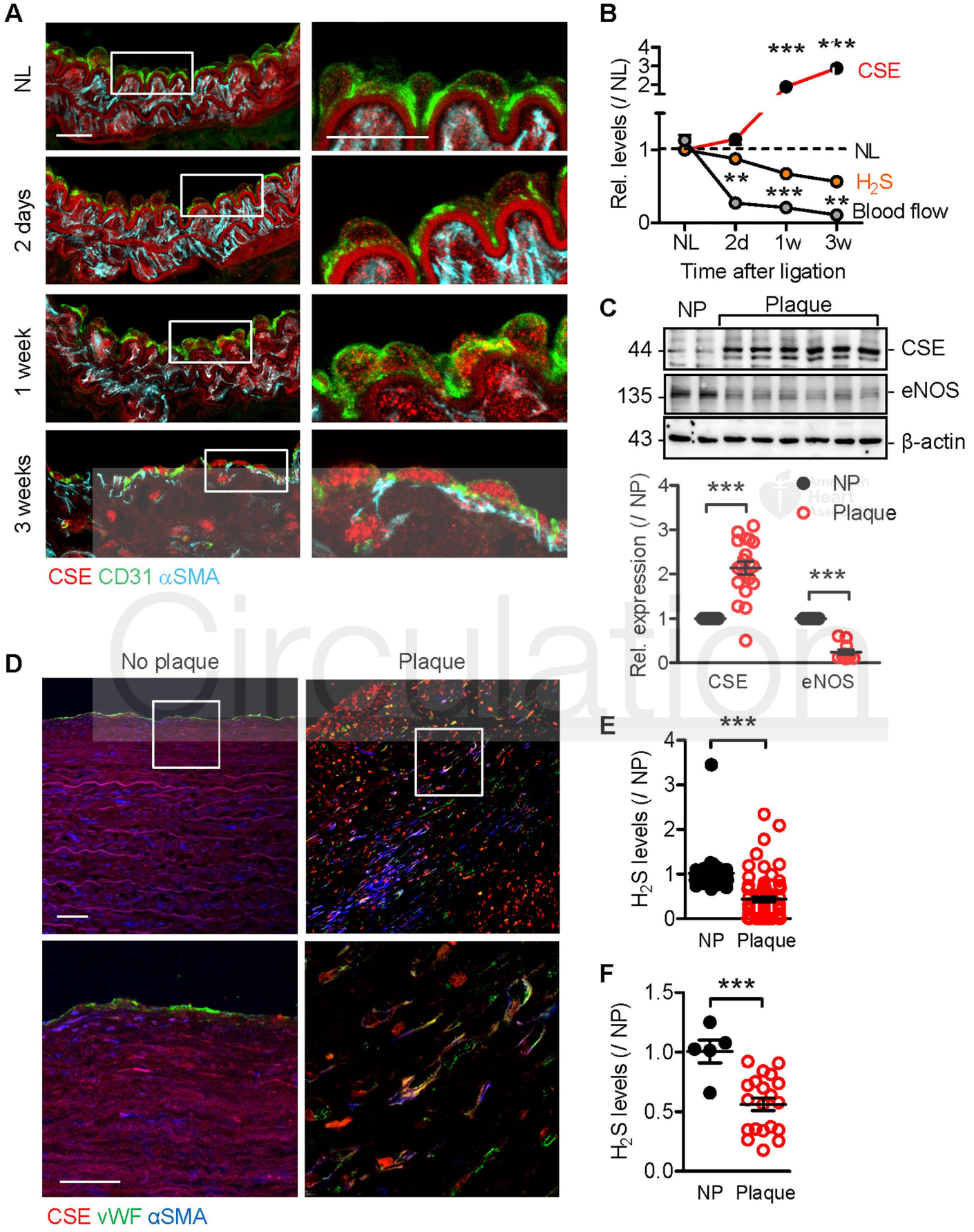

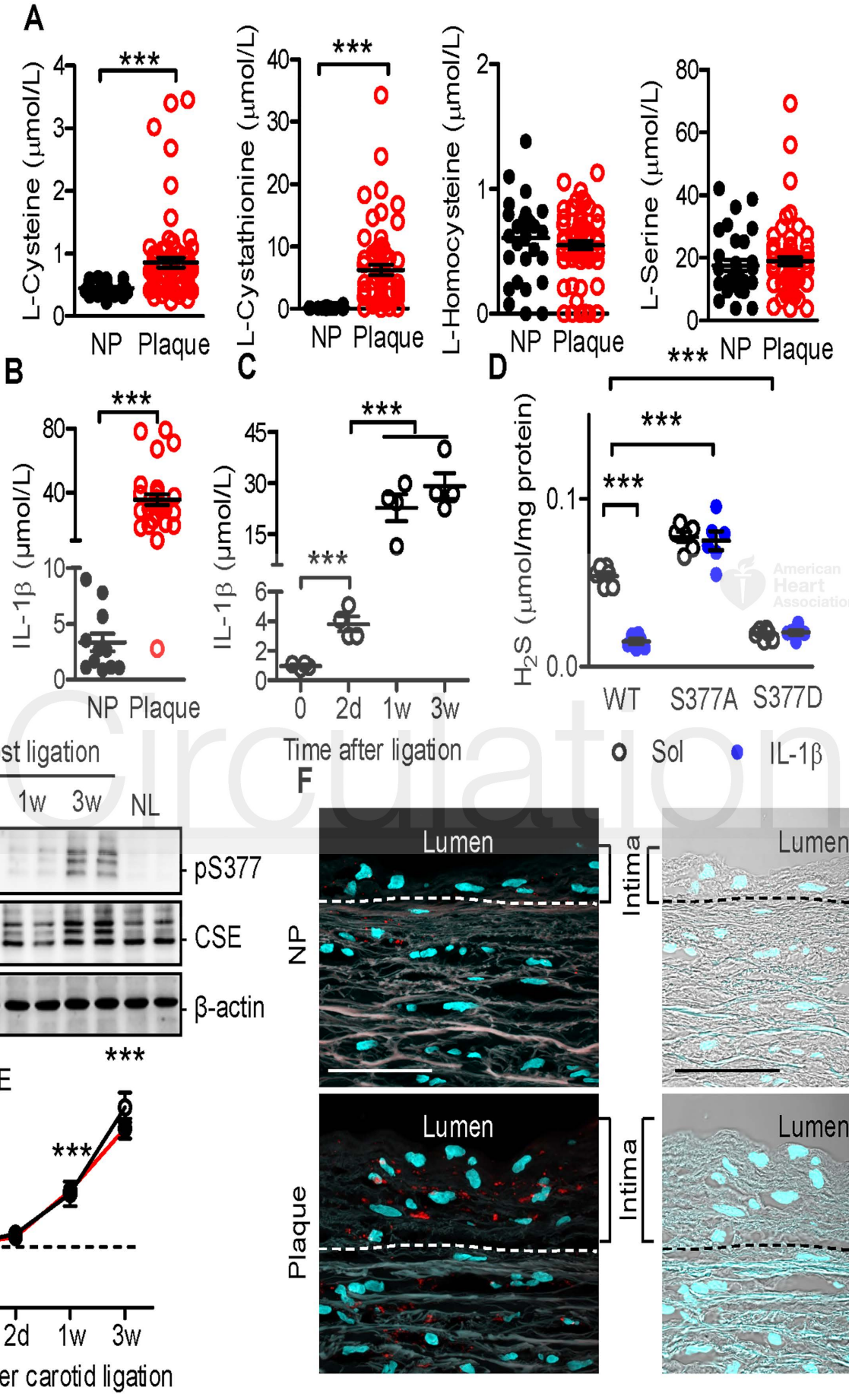

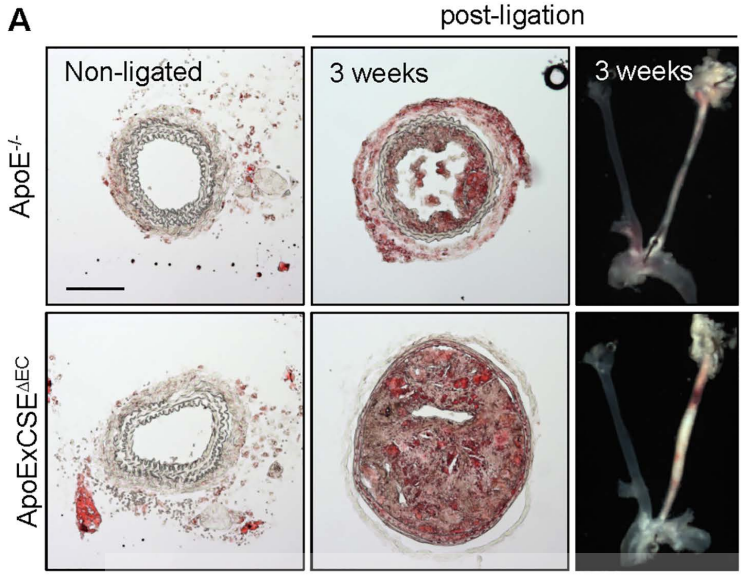

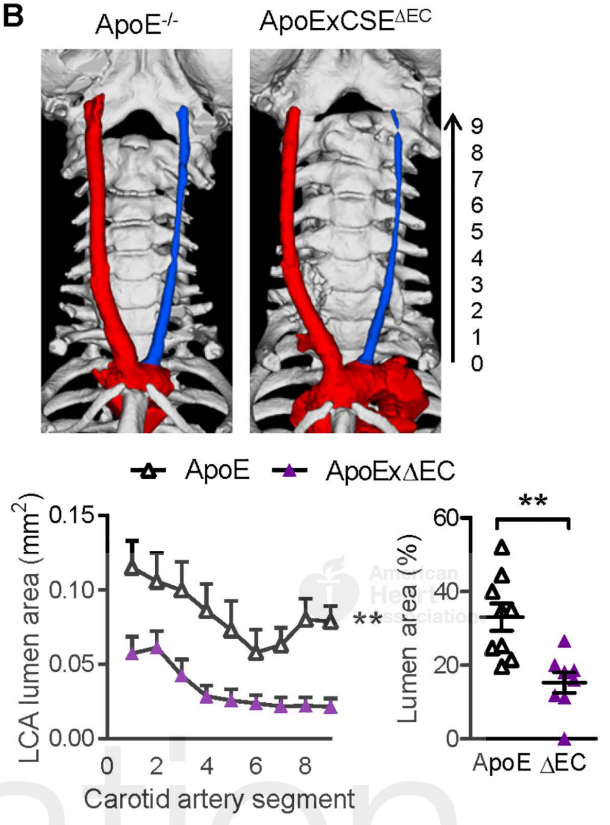

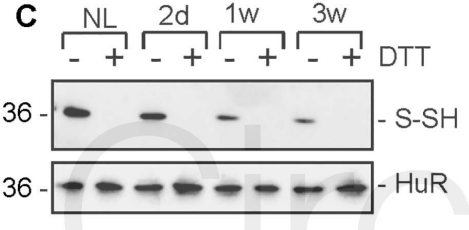

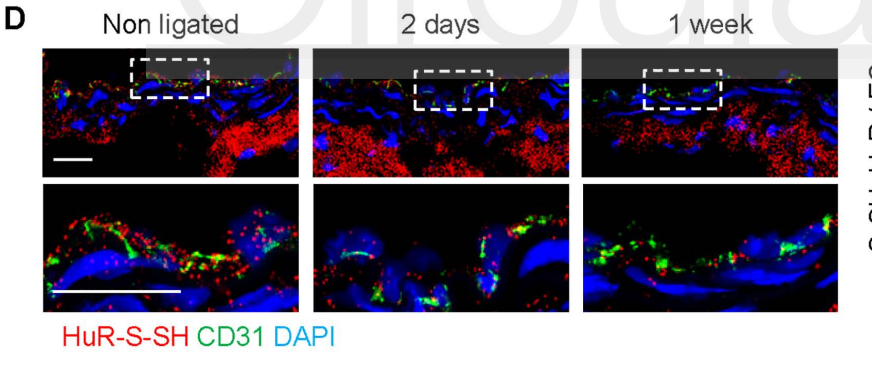

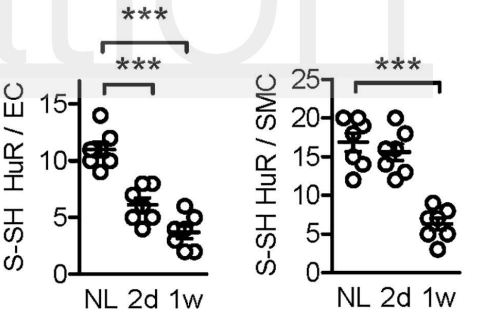

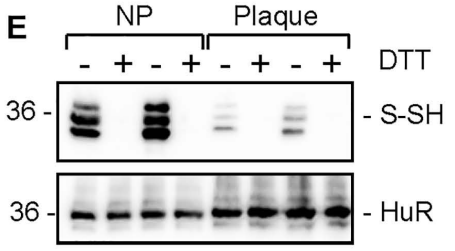

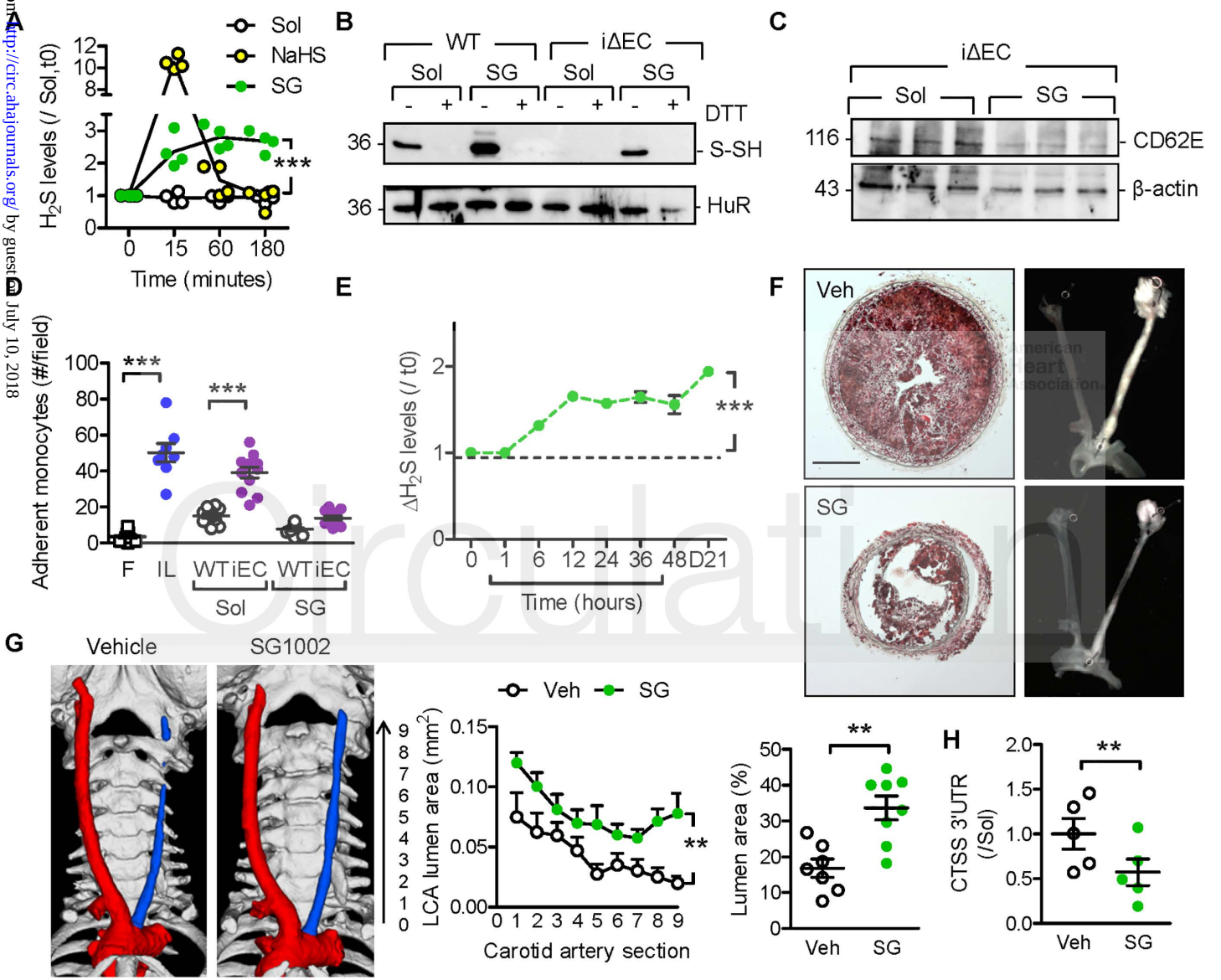

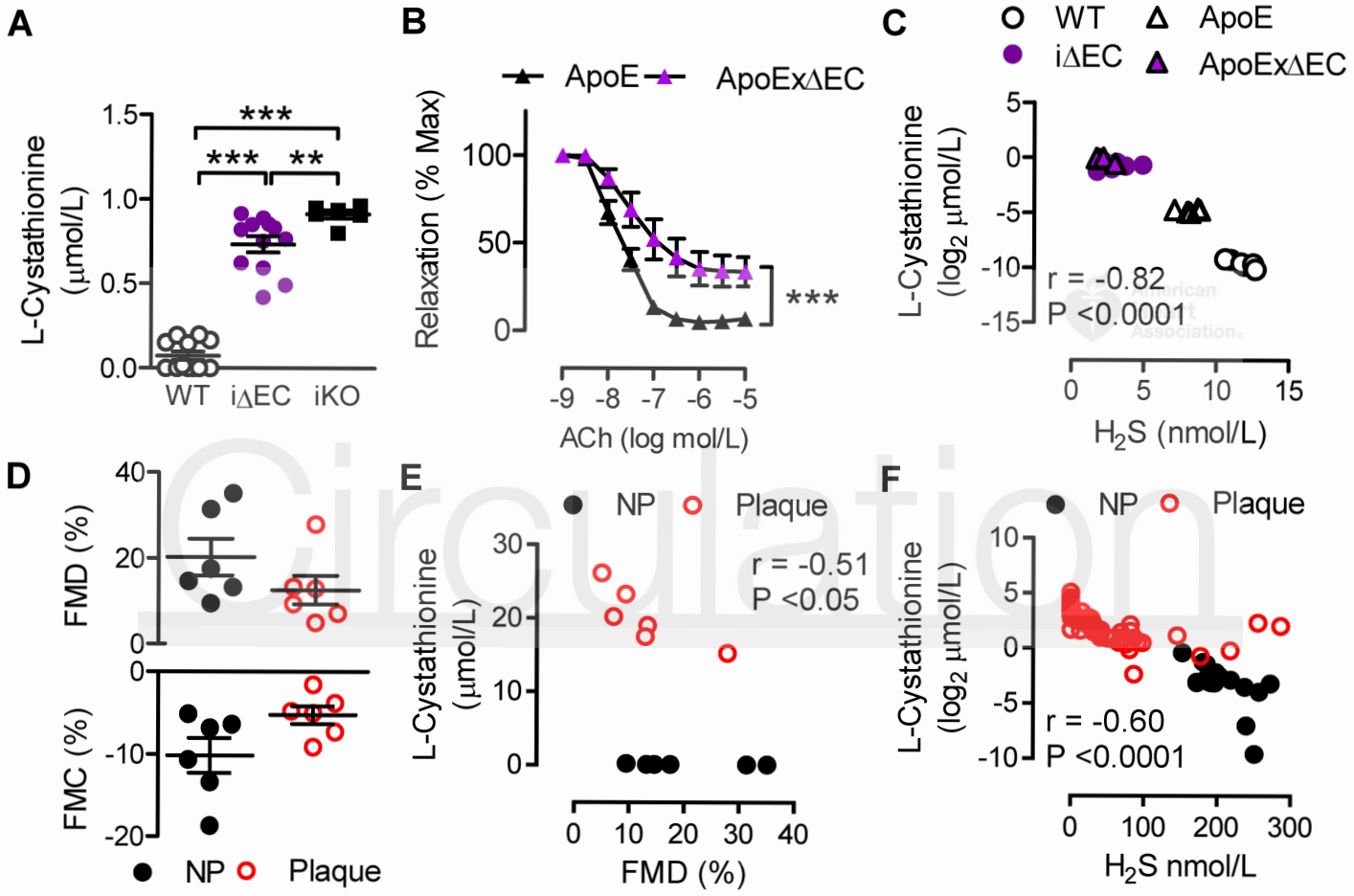

Cystathionine γ Lyase Sulfhydrates the RNA Binding Protein HuR to Preserve Endothelial Cell Function and Delay Atherogenesis

Sofia-Iris Bibli, Jiong Hu, Frangiska Sigala, Ilka Wittig, Juliana Heidler, Sven Zukunft, Diamantis I. Tsilimigras, Voahanginirina Randriamboavonjy, Janina Wittig, Baktybek Kojonazarov, Christoph Schürmann, Mauro Siragusa, Daniel Siuda, Bert Luck, Randa Abdel Malik, Konstantinos A. Filis, George Zografos, Chen Chen, Dao Wen Wang, Josef Pfeilschifter, Ralf P. Brandes, Csaba Szabo, Andreas Papapetropoulos and Ingrid Fleming

Circulation. published online July 3, 2018;
Circulation is published by the American Heart Association, 7272 Greenville Avenue, Dallas, TX 75231

Print ISSN: 0009-7322. Online ISSN: 1524-4539

SUPPLEMENTAL MATERIAL

Cystathionine γ lyase sulfhydrates the RNA binding protein HuR to preserve endothelial cell function and delay atherosclerosis development

Materials and Methods

Materials

Cell culture media were from Gibco (Invitrogen; Darmstadt, Germany). OCT Tissue Tek was from Sakura (Staufen, Germany) and the protease inhibitor cocktail was from Roche (Mannheim, Germany). Sulfane Sulfur Probe 4 (SSP4) was from Dojindo (GERBU Biotechnik GmbH, Heidelberg, Germany) and both interleukin (IL)-1β and the rabbit anti-CSE antibody were from Proteintech (Manchester, UK). Actinomycin D, the β-actin and the Cy3-conjugated α smooth muscle actin antibodies and all other chemicals (unless otherwise specified), were from Sigma-Aldrich (Darmstadt, Germany).

The antibodies against CD31 (rat), CD62E (rabbit) and eNOS (mouse) were from BD Transduction (Heidelberg, Germany), the CD144 (goat) and HuR (mouse) antibodies were from Santa Cruz (Heidelberg, Germany), the Von Willebrand factor (sheep) and the V5 (rabbit) antibodies were from Abcam (Cambridge, UK), anti-CBS (rabbit) was from Abnova (Biozol, Echnig, Germany), and anti-3MST (rabbit) was from Atlas (Bromma, Sweden). The phospho-serine (mouse) antibody was from Biomol GmbH (Hamburg, Germany), the phospho-tyrosine (mouse) antibody was from Millipore (Merck, Darmstadt, Germany) and the phospho-threonine (rabbit) antibody was from Cell Signaling Technologies (Europe B.V., Frankfurt, Germany). The phospho-specific S377 CSE (rabbit) antibody was raised by Pacific Immunology Corp (Ramona, CA). Secondary antibodies were from Calbiochem (Darmstadt, Germany). The PE-CD62E and APC-CD144 antibodies used for FACS analysis were from Biolegend (Koblenz, Germany). Alexa fluor secondary antibodies and Phalloidin were from Thermo Scientific (Dreieich, Germany).

Animals

Floxed CSE ($CSE^{fl/fl}$) mice were generated as described[1], and crossed with tamoxifen-inducible Cdh5-CreERT2 mice[2] in the C57/BL6J background or with Cdh5-Cre mice in the apolipoprotein E-deficient ($ApoE^{-/-}$) background; $ApoE^{-/-}$ mice were originally purchased from Charles River Laboratories Sulzfeld, Germany. Mice were housed in conditions that conform to the *Guide for the Care and Use of Laboratory Animals* published by the U.S. National Institutes of Health (NIH publication no. 85-23). Animals received the usual laboratory diet and all studies were approved by the animal research ethics committees in Athens (790/13-02-2014) and Darmstadt (FU1177 and FU1189). Littermates of both genders were used. To induce robust Cre activity, animals were treated with tamoxifen (75 mg/kg i.p., Sigma-Aldrich) for 5 days. Sufficient knock down of CSE was observed 7 days post-injection.

Partial carotid artery ligation

Animals were randomized following the block randomization method to ensure similar sample sizes per group. Groups were age and sex matched. Experiments were performed in a double blinded manner. Partial ligation of the left carotid artery was performed as described[3]. Briefly, anesthesia was induced by intraperitoneal injection of a mixture of xylazine (5 mg/kg) and ketamine (100 mg/kg). The left carotid artery was exposed by blunt dissection and three of the four caudal branches (left external carotid, internal carotid and occipital artery) were ligated with a 6.0 silk suture while the superior thyroid artery was left intact. A single subcutaneous injection of buprenorphine (0.05 mg/kg) was given 30 minutes prior to and 4-6 hours after partial ligation (plus twice a day for consecutive two days) for pain relief. Post-operative animals were monitored for wealthness every day and their body weight was monitored weekly. For atherosclerosis studies, mice were fed a Paigen diet (energy 35 kJ% fat, containing 12.5 mg/kg cholesterol) immediately following partial ligation until the end of the experiments i.e. 2 days, one or three weeks after ligation. Ligated left carotid arteries and non-ligated right carotid arteries were used for immunostaining studies. Rescue studies

were perform with the addition of sodium polysulthionate (SG1002, Sulfagenix Inc, USA) 400-600 ng/day in the drinking water starting one day prior to partial carotid ligation. Exclusion criteria included post-operative death (0 animal excluded in the end of the study) and negative flox or cre genotype (1 animal excluded as was found CSE flox negative after re-genotyping).

Ultrasound imaging of the carotid arteries

Anesthesia was induced and maintained using isoflurane (induction 3%, maintenance 1.0–1.5% in room air supplemented with 100% O_2) delivered using a vaporizer (Visualsonics, Toronto, Canada). Mice were placed on a heating platform and limbs were taped to electrocardiogram electrodes to monitor heart rate. Body temperature was monitored using a rectal thermometer (Indus Instruments, Houston, TX). The neck area of each mouse was shaved and treated with a chemical hair remover to reduce ultrasound attenuation. To provide a coupling medium for the transducer, a pre-warmed ultrasound gel was spread over the neck area. Blood flow velocity of the left and right carotid arteries was measured using the Vevo3100 imaging system equipped with a 32-55 MHz transducer (MX550D, Visualsonics, Canada) in pulse wave Doppler mode 2, 7 and 21 days after surgery. The peak systolic velocity was calculated offline by an experienced sonographer using the VisualSonics Vevo3100 system.

***In vivo* microCT**

Experiments were performed as described previously[4]. In brief, animals were anesthetized with isoflurance (1%) and the neck was fixed by polystyrene foam. AuroVist (100 µl/28g bodyweight - nanoparticles 15 nm; Nanoprobes, NY, USA) was injected into the tail vein and a 13 minute scan was performed with the following settings: 50 kV, aluminium 1 mm filter, 250 µA source current, exposure time 750 ms, 18 µm isotopic resolution, 1 projection image per 0.5° gentry rotation step, rotation range 360° and a field of view covering the neck region (microCT, Skyscan. Kontich, Germany). Data were reconstructed with the NRecon/ InstaRecon CBR Server – Premium software (Skyscan, Kontich, Belgium/ InstaRecon, Champaign, Illinois, USA). Image analysis, segmentation and quantification of carotid artery lumen area were performed with the Imalytics Preclinical Software (Gremse-IT, Aachen, Germany). Discrimination of contrast agent and soft tissue was achieved by applying a fixed threshold. The lumen areas along the carotid arteries were calculated with the virtual elastic sphere tool and averaged over nine equidistant parts. The start point was set shortly behind the aorta in the carotid artery and the end point shortly before the bifurcation. For demonstration purpose, 3D-Models were fit to scale and freed of artefacts with Imalytics Preclinical.

Vascular reactivity studies

Vascular function was assessed as previously described[5]. Aorta from ApoE and ApoExCSE$^{\Delta EC}$ mice were cleaned of fat and connective tissue, and cut into 2 mm long segments. The presence of a functional endothelium was assessed in all preparations by the ability of acetylcholine (1 µmol/L) to induce more than 60% relaxation of vessels pre-contracted with phenylephrine (1 µmol/L) and only arteries with an intact endothelium were used for further studies. A concentration-relaxation curve to acetylcholine was generated using arteries pre-contracted to 80% of their maximal response to phenylephrine in the presence of the cyclooxygenase inhibitor diclofenac (10 µmol/L).

Cell isolation and culture

Human umbilical vein endothelial cells were isolated and cultured as described[6], and confluent cells up to passage 2 were used for the different experiments. The use of human material in this study conforms to the principles outlined in the Declaration of Helsinki and the isolation of endothelial cells was approved in written form by the ethics committee of the Goethe University Hospital.

Murine lung endothelial cells were isolated from wild-type or $CSE^{i\Delta EC}$ mice, cultured as described[7] and used up to passage 8. To induce CSE deletion *in vitro,* cells (passage 5-6) were treated with 4-OH-tamoxifen (10 µmol/L) for 7 days. Tamoxifen was removed and the cells passaged a further 2-3 times before experiments were performed. Cells isolated from wild-type mice were treated identically.

HEK-293 were cultured in MEM containing 8% heat inactivated FCS, gentamycin (25 µg/mL), non-essential amino acids (MEM NEA, Thermo Fisher Scientific, Schwerte, Germany) and Na pyruvate (1 mmol/L). Cultures were kept in a humidified incubator at 37°C containing 5% CO2. THP-1 monocytic cells were purchased from ATCC (VA, USA) and cultured in RPM1 1640 containing 2 mmol/L glutamine; 10 mmol/L HEPES; 1mmol/L sodium pyruvate; 4.5g/L glucose; 1.5g/L sodium bicarbonate and 10% FCS.

Shear stress

Human endothelial cells (1st passage) or murine lung endothelial cells (5th-7th passage) were transferred to culture medium containing 2% FCS and either maintained under static conditions or exposed to shear stress (12 dyne cm^{-2}) in a cone-plate viscosimeter, as described[8].

Cell transfection

Endothelial cells were transfected with small interfering RNAs (siRNA) directed against CSE, HuR, or a scrambled negative control (Eurogentec), using Lipofectamine RNAiMAX (Invitrogen, Karlsruhe, Germany). Cells were then kept in culture for a further 48 hours.

Adenoviral transduction

GFP and CSE adenoviruses were generated as described [9,10]. Adenoviruses (10 MOI) were incubated with AdenoBoost (Sirion Biotech, Martinsried, Germany) for 30 minutes before being added to endothelial cells (80% confluent) in EGM containing 0.1% BSA for 4 hours at 37°C. Cells were then washed, and cultured for an additional 36 hours in the presence of 20% FCS.

Cell adhesion

Endothelial cells (cultured in 96 well plates) were stimulated with IL-1β (30 ng/ml, 3 hours). Thereafter, THP-1 cells (100.000) were added and left undisturbed for 30 minutes. Thereafter, non-adherent cells were removed by gentle washing and adherent cells were imaged. In some studies a control purified mouse IgG1 and a purified anti-mouse CD62E neutralizing antibody (1:200; Biolegend, Koblenz, Germany) were included.

Generation of point mutants

Mutations of CSE and HuR were generated using a QuickChange kit (Stratagene, Waldbronn, Germany) with point mutation primers for Ser377 and S282 to alanine or aspartic acid, Y60 and Y114 to phenylalanine or aspartic acid for CSE, or cysteine to alanine at positions 13, 245 and 284 for HuR.

Cell transfection

HEK-293 cells were transfected with pcDNA 3.1, CSE, myc-WT CSE, myc-S377A CSE, myc-S377D CSE, WT HuR, C13A HuR, C245A HuR and C284A HuR plasmids using Lipofectamine 2000 (Invitrogen, Karlsruhe, Germany) according to the manufacturer's instructions. Cells were then maintained in culture and studied 24 hours after transfection. In the case of HuR transfection in HEK-293 cells, endogenous HuR levels were silenced by adding a small interfering RNA directed against HuR (in the presence of Lipofectamine RNAimax) 72 hours prior to transfection. Cells transfected with a control oligonucleotide were used as a positive control.

Immunohistochemistry

Wild-type or $CSE^{i\Delta EC}$ aortae were embedded in OCT Tissue TeK (Sakura, Staufen, Germany) and frozen on dry ice. Subsequently, sections (6 µm) were prepared on a microtome (Microm HM 650, Thermo Scientific, Darmstadt, Germany) and placed on positively charged glass slides. The samples were re-hydrated with phosphate–buffered saline (PBS) for 5 minutes and incubated for 2 hours at room temperature (RT) in a blocking buffer consisting of Triton X-100 (0.3%), horse serum (5%) and BSA (0.5%) in PBS. Samples were washed with PBS and primary antibodies against CSE and CD31 were added in final dilution of 1:500 in Triton X-100 (0.2% in PBS) overnight at 4°C. Thereafter, secondary antibodies against rabbit and rat were diluted 1:200 in PBS supplemented with DAPI (10 ng/ml) and a Cy3-congugated anti α-smooth muscle actin antibody (1:500). After washing, sections were mounted with Dako fluorescent mounting medium (Dako, Glostrup, Denmark).

Ligated and non-ligated carotid were dissected, perfused with PBS and fixed in 4% paraformaldehyde overnight. Samples were stained with oil O red for evaluation of intima-media ratio.

For *en face* immunostaining, whole aortae from wild-type or $CSE^{i\Delta EC}$ were cleaned of perivascular fat and fixed for 30 minutes at room temperature with 4% paraformaldehyde (PFA) before blocking and staining with antibodies against CSE and CD144 as described above. In some experiments, the surface expression of CD144 and CD62E was determined in non-permeabilized samples i.e. Triton X-100 was omitted from the buffers. Human samples were fixed in 4% paraformaldehyde and sectioned in paraffin. After demasking with sodium citrate buffer (10 mmol/L, pH 6.0), staining was performed as for the murine samples.

Proximity ligation was performed using the Duolink assay according to manufacturer's instructions (Sigma), usign antibodies against phosphoserine (mouse) and CSE (rabbit). Images were taken using a confocal microscope (LSM-780; Zeiss, Jena, Germany) and ZEN software (Zeiss).

Modified *in situ* biotin switch assay-proximity ligation assay

For the modified *in situ* biotin switch assay-proximity ligation assay, samples of carotid artery were permeabilized with Triton X-100 (1%) followed by blocking of free thiols with methane thiosulfonate (MMTS, 20 mmol/L). Thereafter, sulfhydrated proteins were labeled with the iodoacetyl-PEG2-biotin diluted in phosphate buffer saline solution at a final concentration of 10 mg/ml. After 5 washing steps of 30 minutes with phosphate buffer saline (pH=7.4), samples were blocked with the Duolink buffer (Sigma) and incubated with antibodies against biotin (rabbit), HuR (mouse), CD31 (rat) and Cy-α-smooth muscle actin. Proximity ligation was performed according to manufacturer's instructions.

Immunoblotting

Samples (cells or tissues) were lysed in ice-cold RIPA buffer (50 mmol/L Tris HCl-pH 7.5, 150 mmol/L NaCl, 25 mmol/L NaF, 10 mmol/L $Na_4P_2O_7$, 1% Triton X-100 and 0.5% sodium deoxycholate) supplemented with 0.1% SDS and protease and phosphatase inhibitors. Protein concentrations were determined using the Bradford assay, and detergent-soluble proteins were solubilized in SDS-PAGE sample buffer, separated by SDS-PAGE and subjected to Western blotting as described[7]. Proteins were visualized by enhanced chemiluminescence using a commercially available kit (Amersham, Freiburg, Germany).

Human samples were lysed in ice-cold RIPA buffer supplemented with 0.1% SDS as well as protease and phosphatase inhibitors. Proteins were then precipitated in acetone (4/1 v/v) overnight at -80°C. Following centrifugation (16000 g, 15 minutes, 4°C) the pellets were re-suspended in ice cold RIPA buffer containing 1% SDS and protease and phosphatase inhibitors. Samples (1 mg/ml) were passed through desalting columns (Thermo Scientific) and the recovered proteins were used for subsequent evaluation. Proteins were separated by SDS-PAGE and subjected to Western blotting.

To evaluate the dimeric form of HuR or the tetrameric form of CSE, samples were lysed in non-reducing non-denaturating conditions using RIPA buffer without the addition of SDS and

boiled in a DTT free Laemli lysis buffer. Western blotting was performed in the absence of SDS at 4°C.

Immunoprecipitation of CSE

Samples were lysed in a HEPES lysis buffer (20 mmol/L HEPES pH 7.5, 1.5 mmol/L $MgCl_2$, 5 mmol/L EGTA, 150 mmol/L NaCl, 1% Triton X-100, 0.5% glycerol buffer containing a protease inhibitor cocktail). After centrifugation at 16,000xg for 15 minutes supernatants were pre-incubated with protein G agarose beads (Pierce, IL, USA) for 2 hours. Supernatants were incubated with protein G agarose beads coated with antibody against V5 or CSE overnight at 4°C. Samples were washed with lysis buffer and analyzed by SDS–PAGE or washed 3 times with HEPES lysis buffer without Triton X-100 and glycerol and evaluated in mass spectrometry for interactions.

IL-1β ELISA

Circulating levels of IL-1β were evaluated with a commercially available kit according to manufactures instructions (R&D, Invitrogen).

Sample preparation for the identification of CSE-interacting proteins

Beads were resuspended in 50 µl 6M guanidine hydrochloride (GdmCl), 50 mmol/L Tris/HCl, pH 8.5 and incubated at 95°C for 5 minutes. Samples were diluted with 25 mmol/L Tris/HCl, pH 8.5, 10% acetonitrile to obtain a final GdmCl concentration of 0.6 mol/L. Proteins were digested with 1 µg Trypsin (sequencing grade, Promega) overnight at 37°C under gentle agitation. Digestion was stopped by adding trifluoroacetic acid to a final concentration of 0.5%. Peptides were loaded on multi-stop-and-go tip (StageTip) containing three strong cation exchange (SCX) disks and a stack of three C18-disks on top. SCX fractionation by StageTips was performed as described[11]**.** Three fractions of each sample were eluted in wells of microtiter plates and peptides were dried and resolved in 1% acetonitrile, 0.1 % formic acid.

Mass spectrometry of CSE interacting proteins

Liquid chromatography/mass spectrometry (LC/MS) was performed using a Thermo Scientific™ Q Exactive Plus equipped with an ultra-high performance liquid chromatography unit (Thermo Scientific Dionex Ultimate 3000) and a Nanospray Flex Ion-Source (Thermo Scientific). Peptides were loaded on a C18 reversed-phase pre-column (Thermo Scientific) followed by separation on a 2.4 µm Reprosil C18 resin (Dr. Maisch GmbH) in-house packed picotip emitter tip (diameter 100 µm, 15 cm long from New Objectives) using a gradient from mobile phase A (4% acetonitrile, 0.1% formic acid) to a 30 % mobile phase B (99% acetonitrile, 0.1% formic acid) for 25 minutes followed by a second step to 60% B for 5 minutes (IP). MS data were recorded by data dependent acquisition Top10 method for HCD fragmentation in positive mode. Lock mass option was enabled to ensure high mass accuracy between multiple runs. The full MS scan range was 300 to 2000 m/z with resolution of 70000, and an automatic gain control (AGC) value of $3x10^6$ total ion counts with a maximal ion injection time of 160 ms. Only higher charged ions (2+) were selected for MS/MS scans with a resolution of 17500, an isolation window of 2 m/z and an automatic gain control value set to 10^5 ions with a maximal ion injection time of 150 ms. Selected ions were excluded in a time frame of 30 s. Fullscan data were acquired in profile and fragments in centroid mode.

Data analysis for CSE interacting proteins

For data analysis MaxQuant 1.5.3.30 (Cox and Mann, 2008, Nat. Biotechnology), Perseus 1.5.6.0[12] and Excel (Microsoft Office 2013) were used. For protein immunoprecipitation experiments the following settings were used: N-terminal acetylation (+42.01), oxidation of methionine (+15.99) and carbamidomethylation (+57.02) on cysteines were selected as modifications. The mouse reference proteome set (Uniprot, February 2016, 79950 entries supplemented with the human CTH, P32929) was used to identify peptides and proteins with a false discovery rate (FDR) less than 1%. Minimal ratio count for label-free quantification was 2. Reverse identifications and common contaminants were removed and the data-set

was reduced to proteins that were identified in all 5 samples in one experimental group. Missing values were replaced by a background value which reflects the smallest value of data set. Significant interacting proteins were determined by permutation-based FDR calculation.

RNA Immunoprecipitation

Endogenous RIP studies were performed using the MagnaRIP Kit according to the manufacturer's protocol (Millipore). Briefly, to cross-link RNA and proteins, cells or tissues were treated with formaldehyde (0.1% in PBS) at 4 °C for 30 minutes and subsequently lysed with RIP lysis buffer for 40 minutes on ice. The whole-cell lysates were incubated at 4 °C overnight with magnetic protein A–protein G beads coupled with 5 µg of either normal mouse IgG (Millipore) or HuR monoclonal antibody (mouse monoclonal antibody; clone: 3A2, sc-5261, Santa Cruz Biotechnology, Inc.). Beads were then washed three times followed by RNA isolation from the immunoprecipitates. cDNA was prepared in each case as described above. RT–qPCR was performed by amplifying a 300bp region in the 3′ UTR of both CTSS transcript variants and CD62E (primers presented on the qPCR section). To ensure efficient binding of the antibody to its antigen, the presence of the HuR protein was monitored in the post-immunoprecipitation supernatant as well as in the immunoprecipitate.

Sulfhydration

Sulfhydration was detected using a modified biotin switch assay. In brief, samples were precipitated with 20% trichloroacetic acid (TCA) and stored at -80^{o}C. Precipitates were washed with 10% and then 5% TCA and then centrifuged (16000g, 30 minutes, 4°C) before being suspended in HENs buffer (250 mmol/L HEPES-NaOH, 1 mmol/L EDTA, 0.1 mmol/L neocuproine, 100 µmol/L deferoxamine, 2,5% SDS) containing 20 mmol/L methanethiosulfonate (MMTS) to block free thiols and protease and phosphatase inhibitors. Acetone precipitation was performed and pellets were re-suspended in 300 µL qPerS-SID lysis buffer (6 mol/L urea, 100 mmol/L NaCl, 2 % SDS, 5 mmol/L EDTA, 200 mmol/L Tris pH 8.2; 50 mmol/L iodoacetyl-PEG2-biotin, 2.5 mmol/L dimedone), sonicated and incubated for 2 hours at room temperature in the dark. Lysates (500 µg) were precipitated with acetone and protein pellets were re-suspended in 50 µl Tris/HCl (50 mmol/L, pH 8.5) containing guanidinium chloride (GdmCl 6 mmol/L), and incubated at 95°C for 5 minutes. A negative control was generated for each sample by adding DTT (1 mmol/L) during biotin cross-linking. Biotin was then immunoprecipitated overnight (4^{o}C) using a high capacity streptavidin resin (Thermo Scientific, Heidelberg, Germany). Elution was performed by addition of 3% SDS, 1% β-mercaptoethanol, 8 mol/L Urea and 0.005% bromophenol blue in PBS for 15 minutes at room temperature followed by 15 minutes at 95^{o}C. Sulfhydrated proteins were then detected by SDS PAGE and Western blotting.

Enzymatic purification and activity of CSE mutants

Wild-type or mutated GST-CSE were purified and the activity evaluated using the methylene blue assay, as described[13].

H_2S measurements.

Intracellular levels of H_2S were measured by monitoring the selective reaction of SSP4 with H_2S. In brief, cells were seeded in 12 or 48 well plates and cultured to confluency. The culture medium was replaced with phenol red-free Endothelial Growth Medium (EGM, PeloBiotech, Martinsried, Germany) supplemented with 0.1 % BSA. After 2 hours, SSP4 (10 µmol/L), L-cysteine (100 µmol/L) and pyridoxal phosphate (10 µmol/L) were added for 60 minutes. In case of tissues substrates and co-factors were added for 60 minutes in homogenates of 1 mg/ml protein in 1% Triton X-100 lysis buffer supplemented with protease and phosphatase inhibitors. Samples were incubated for 60 minutes at 37^{o}C. Thereafter, the tissue supernatant or cell supernatant was collected and floating cells were removed by centrifugation (16000 g, 10 minutes, 4°C). The specific products of the reaction of H_2S with SPP4 were quantified by LC-MS/MS.

Nitrite measurements

Plasma samples from ApoExCSE$^{\Delta EC}$ mice 21 days after carotid artery ligation were prepared as described[14]. Circulating nitrites were measured using a Nitric Oxide Analyzer (Sievers 280_max 1150W, GE Analytical Instruments, Colorado, USA) after reaction with iodide and acetic acid under nitrogen at room temperature.

FACS analyses

Murine endothelial cells were treated with solvent or IL-1β (30 ng/ml, 4 hours). After washing, cells were re-suspended in PBS and labeled with a PE-conjugated anti-CD62E antibody and an APC-conjugated anti-CD144 Biolegend (Koblenz, Germany). The cell suspension was washed, re-suspended in PBS and analyzed in a FACscan flow cytometer using the CellQuest software (Becton Dickinson, CA, USA).

RT-qPCR

Total RNA was extracted using an RNeasy kit (QIAGEN, Hilden, Germany) and equal amounts (1 µg) of total RNA were reverse transcribed (Superscript III; Invitrogen). Gene expression levels were detected using SYBR Green (Absolute QPCR SYBR Green Mix; Thermo Fisher Scientifc). The relative expression levels of the different genes studied was calculated using the formula $2^{-\Delta Ct}$ ($\Delta C_t = C_{t\ (gene)} - C_{t\ (housekeeping\ gene)}$) with the 18S RNA as a reference. The primer sequences used were as follows:

18s	forward 5´-CTTTGGTCGCTCGCTCCTC-3´
	reverse 5´-CTGACCGGGTTGGTTTTGAT-3´
hCD62E	forward 5´- CCGAGCGAGGCTACATG AAT-3´
	reverse 5´- GCCAGAGGAGAAATGGTGCT-3´
mCD62E	forward 5´- ATGGAAGCCTGAACTGCTCC-3´
	reverse 5´- CCATTCCCCTCTTGGACCAC-3´
hCSE	forward 5´- ACTTCAGGCAAGTGGCATCTG-3´
	reverse 5´- GCCAAAGGGCGCTTGGTTT-3´
mCSE	forward 5´- AGGGTGGCATCTGAATTTGG-3´
	reverse 5´- GTTGGGTTTGTGGGTGTTTC-3´
ICAM-1	forward 5´- CTTCCAGCTACCATCCCAAA-3´
	reverse 5´- CTTCAGAGGCAGGAAACAGG -3´
VCAM-1	forward 5´- CAATGGGGTGGTAAGGAATG-3´
	reverse 5´- ACCTCCACCTGGGTTCTCTT-3´
eNOS	forward 5´- GCTGTTCCAGATTCG-3´
	reverse 5´- GCTGCAGGTGTTCGATG-3´
3'UTR CTSS	forward 5´- GGCTCCTTCTCCATAAAGCA-3´
	reverse 5´- AAAGTAGGCTGGGCTCAGTG -3´

mRNA stability assay

The decay rate of CD62E mRNA was assessed at regular intervals following transcriptional inhibition using actinomycin D. Briefly, endothelial cells from wild-type or CSE$^{i\Delta EC}$ mice were treated with actinomycin D (1 µg/mL) for up to 24 hours. RNA was then extracted and levels of *CD62E* mRNA were determined by RT–qPCR. Residual mRNA levels were calculated based on the mathematical formula $2^{(-Ct(gene,\ \text{each time point}) + Ct(gene,\text{time point 0}))}$.

Human Samples

Carotid plaques were prospectively collected from 24 random patients, who had internal carotid artery (ICA) stenosis of 75-90% and underwent carotid endarterectomy (see **Table I** for details of the study cohort). Arteriographical evaluation of the carotid bifurcation stenosis was performed and the degree of luminal stenosis was determined according to North American Symptomatic Carotid Endarterectomy Trial (NASCET) criteria. Peal systolic velocity was monitored by using a Philips HD11 ultrasound platform (Philips, Netherlands). Eight additional samples of healthy thyroid arteries were used as the control group. Thyroid arteries were chosen from aged matched subjects without additional comorbidities as described in **Table I**. Samples were collected post-mortem and were evaluated by a pathologist for the possibility of atherosclerotic lesions. Arteries that showed no pathological characteristics were snap frozen for additional analysis. Tissue samples were either frozen and used for biochemical analyses or embedded in paraffin for immunostaining purposes.

Plasma from a further 70 patients characterized with internal carotid artery stenosis of 75-90% before carotid endarterectomy and 32 age matched healthy donors was used for the amino acid profiling, H_2S measurements and assay of IL-1β levels (see **Supplemental Table 2** for details of the study cohort).

All studies followed the Code of Ethics of the World Medical Association (Declaration of Helsinki). The study protocols were approved by the Institutional Ethics Committee (Scientific and Ethic Committee of Hipokrateion University Hospital, PN1539) and all patients enrolled gave their informed consent.

Assessment of endothelial function in humans

Flow-mediated dilation (FMD) and low-flow-mediated constriction (L-FMC) were measured in 12 subjects; 6 with atherosclerosis and 6 without (**Supplemental Table 6**), as described[15]. L-FMC corresponds to the constriction observed during a 4.5 minute occlusion of a pneumatic cuff placed distal to the site of arterial diameter measurement. FMD corresponds to the maximal dilation observed in the 5 minutes following deflation of the cuff, i.e. during reactive hyperaemia. All data were acquired digitally and analyzed in a randomized, blinded fashion. All participants provided informed consent for their participation in the study, which was approved by the Scientific and Ethic Committee of Hipokrateion University Hospital (extension to PN1539).

Amino acid profiling in plasma and arterial samples

Blood samples from the subjects participating in endothelial function studies were used for amino acid profiling. Sample preparation was performed using the EZ:faast LC-MS free amino acid analysis kit (Phenomenex, Aschaffenburg, Germany) according to the manufacturer's instructions, with minor modifications. Internal standards (10 µl) were applied to all samples and to the standard curve. Sample pH was adjusted to be between pH 1.5-6.0 with hydrochloric acid. Analysis of metabolites was performed by LC-MS/MS using the EZ:faast AAA-MS HPLC column (inner diameter 2 mm) on an Agilent 1290 Infinity LC system (Agilent, Waldbronn, Germany) coupled to a QTrap 5500 mass spectrometer (Sciex, Darmstadt, Germany). Electro spray ionization in positive mode was employed. The intensity of the measured metabolite was normalized to internal standards. Analyst 1.6.2 and MultiQuant 3.0 (Sciex, Darmstadt, Germany), were used for data acquisition and analysis, respectively.

Statistics

Data are expressed as mean ± SEM. Statistical evaluation was performed using Student's t-test for unpaired data. The Mann-Whitney test was used if the sample size was lower than 8 or populations followed non-Gaussian distribution. One-way ANOVA followed by Newman-Keuls test and two-way ANOVA with a Bonferroni post-test were used where appropriate. A linear Pearson model was used for correlation statistics. ANOVA repeated measures with a Bonferroni post test was used where appropriate. Statistical tests are described in the figure

legend for each experiment. Central tendency and dispersion of the data were examined for replicates below 6. Values of $P<0.05$ were considered statistically significant. MetaboAnalyst[16] was used to construct the heat map and perform hierarchical clustering based on amino acid profile.

References

1 Syhr KMJ, Boosen M, Hohmann SW, Longen S, Köhler Y, Pfeilschifter J, Beck KF, Geisslinger G, Schmidtko A, Kallenborn-Gerhardt W. The H_2S-producing enzyme CSE is dispensable for the processing of inflammatory and neuropathic pain. *Brain Res*. 2015;1624:380-389. doi: 10.1016/j.brainres.2015.07.058

2 Monvoisin A, Alva JA, Hofmann JJ, Zovein AC, Lane TF, Iruela-Arispe ML. VE-cadherin-CreERT2 transgenic mouse: a model for inducible recombination in the endothelium. *Dev Dyn*. 2006;235:3413-3422. doi: 10.1002/dvdy.20982

3 Nam D, Ni CW, Rezvan A, Suo J, Budzyn K, Llanos A, Harrison D, Giddens D, Jo H. Partial carotid ligation is a model of acutely induced disturbed flow, leading to rapid endothelial dysfunction and atherosclerosis. *Am J Physiol - Heart Circ Physiol*. 2009;297:H1535-H1543. doi: 10.1152/ajpheart.00510.2009

4 Schürmann C, Gremse F, Jo H, Kiessling F, Brandes RP. Micro-CT technique is well suited for documentation of remodeling processes in murine carotid arteries. *PLoS ONE*. 2015;10:e0130374. doi: 10.1371/journal.pone.0130374

5 Loot AE, Schreiber JG, Fisslthaler B, Fleming I. Angiotensin II impairs endothelial function via tyrosine phosphorylation of the endothelial nitric oxide synthase. *J Exp Med*. 2009;206:2889-2896. doi: 10.1084/jem.20090449

6 Busse R, Lamontagne D. Endothelium-derived bradykinin is responsible for the increase in calcium produced by angiotensin-converting enzyme inhibitors in human endothelial cells. *Naunyn Schmiedebergs Arch Pharmacol*. 1991;344:126-129. doi: 10.1007/BF00167392

7 Fleming I, Fisslthaler B, Dixit M, Busse R. Role of PECAM-1 in the shear-stress-induced activation of Akt and the endothelial nitric oxide synthase (eNOS) in endothelial cells. *J Cell Sci*. 2005;118:4103-4111. doi: 10.1242/jcs.02541

8 Fisslthaler B, Loot AE, Mohamed A, Busse R, Fleming I. Inhibition of endothelial nitric oxide synthase activity by proline-rich tyrosine kinase 2 in response to fluid shear stress and insulin. *Circ Res*. 2008;102:1520-1528. doi: 10.1161/CIRCRESAHA.108.172072

9 Bucci M, Papapetropoulos A, Vellecco V, Zhou Z, Pyriochou A, Roussos C, Roviezzo F, Brancaleone V, Cirino G. Hydrogen sulfide is an endogenous inhibitor of phosphodiesterase activity. *Arterioscler Thromb Vasc Biol*. 2010;30:1998. doi: 10.1161/ATVBAHA.110.209783

10 Coletta C, Papapetropoulos A, Erdelyi K, Olah G, Módis K, Panopoulos P, Asimakopoulou A, Gerö D, Sharina I, Martin E, Szabo C. Hydrogen sulfide and nitric oxide are mutually dependent in the regulation of angiogenesis and endothelium-dependent vasorelaxation. *Proc Natl Acad Sci USA*. 2012;109:9161-9166. doi: 10.1073/pnas.1202916109

11 Rappsilber J, Mann M, Ishihama Y. Protocol for micro-purification, enrichment, pre-fractionation and storage of peptides for proteomics using StageTips. *Nat Protoc*. 2007;2:1896-1906. doi: 10.1038/nprot.2007.261

12 Tyanova S, Temu T, Cox J. The MaxQuant computational platform for mass spectrometry-based shotgun proteomics. *Nat Protoc*. 2016;11:2301-2319. doi: 10.1038/nprot.2016.136

13 Asimakopoulou A, Panopoulos P, Chasapis CT, Coletta C, Zhou Z, Cirino G, Giannis A, Szabo C, Spyroulias GA, Papapetropoulos A. Selectivity of commonly used pharmacological inhibitors for cystathionine β synthase (CBS) and cystathionine γ lyase (CSE). *Br J Parmacol*. 2013;169:922-932. doi: 10.1111/bph.12171

14 Khambata RS, Ghosh SM, Rathod KS, Thevathasan T, Filomena F, Xiao Q, Ahluwalia A. Antiinflammatory actions of inorganic nitrate stabilize the atherosclerotic plaque. *Proc Natl Acad Sci USA*. 2017;114:E550-E559. doi: 10.1073/pnas.1613063114

15 Gori T, Muxel S, Damaske A, Radmacher MC, Fasola F, Schaefer S, Schulz A, Jabs A, Parker JD, Münzel T. Endothelial function assessment: flow-mediated dilation and constriction provide different and complementary information on the presence of coronary artery disease. *Eur Heart J*. 2012;33:363-371. doi: 10.1093/eurheartj/ehr361

16 Xia J, Sinelnikov IV, Han B, Wishart DS. MetaboAnalyst 3.0-making metabolomics more meaningful. *Nucleic Acids Res*. 2015;43:W251-W257. doi: 10.1093/nar/gkv380

Supplemental Table 1. Clinical and demographic data from the studied tissues.

Characteristics	***Plaque subjects***	***NP subjects***
Demographic data		
No.	24	8
Mean age (range)	73.6 (55–86)	65.6 (53–82)
Male /female	14M/10F	6M/2F
Smokers	4	0
Clinical data		
Hypertension	20	0
Diabetes	4	0
Hyperlipidemia	24	0
Coronary disease	0	0
Myocardial Infarction	0	0
Valve insufficiency	0	0
Renal disease	0	0
Heart failure	0	0
Angiographic carotic stenosis		
<90%	24	N/A
Plaque histopathology		
Unstable	12	N/A
Stable	12	N/A
Medication		
Statins	0	0
ACE inhibitors	0	0
β-blockers	0	0

Supplemental Table 2. Clinical and demographic data from the studied plasma.

Characteristics	***Plaque subjects***	***NP subjects***
Demographic data		
No	90	32
Mean age (range)	70.3 (51–87)	64.6 (50–85)
Male /female	60M/30F	20M/12F
Smokers	18	0
Clinical data		
Hypertension	30	0
Diabetes	9	0
Hyperlipidemia	75	0
Coronary disease	34	0
Myocardial Infarction	20	0
Valve insufficiency	0	0
Renal disease	0	0
Heart failure	0	0
Angiographic carotic stenosis		
<90%	90	N/A
Plaque histopathology		
Unstable	45	N/A
Stable	45	N/A
Medication		
Statins	0	0
ACE inhibitors	0	0
β-blockers	0	0

Supplemental Table 3. CSE interacting proteins identified by MS.

Supplemental Table 4. Amino acid profiling of human plasma

Supplemental Table 5. Amino acid profiling from ApoExCSE$^{\Delta EC}$ mice treated with vehicle or SG2001

Supplemental Table 6. Clinical and demographic data from the vascular function studies.

Characteristics	***Plaque subjects***	***NP subjects***
Demographic data		
No	6	6
Mean age (range)	75.8 (57-88)	58.8 (28-76)
Male /female	5M/1F	4M/2F
Smokers	0 (6 ex smokers)	0
Clinical data		
Hypertension	5	0
Diabetes	3	0
Hyperlipidemia	4	0
Coronary disease	2	0
Myocardial Infarction	2	0
Valve insufficiency	0	0
Renal disease	2	0
Heart failure	1	0
Angiographic carotic stenosis		
<90%		N/A
Plaque histopathology		
Unstable	5	N/A
Stable	1	N/A
Medication		
Statins	4	0
ACE inhibitors	1	0
b-blockers	2	0
Blood flow at rest, mL/min	56 ± 4	56 ± 7
During cuff inflation	12 ± 1	12 ± 1
After cuff deflation	131 ± 9	120 ± 7

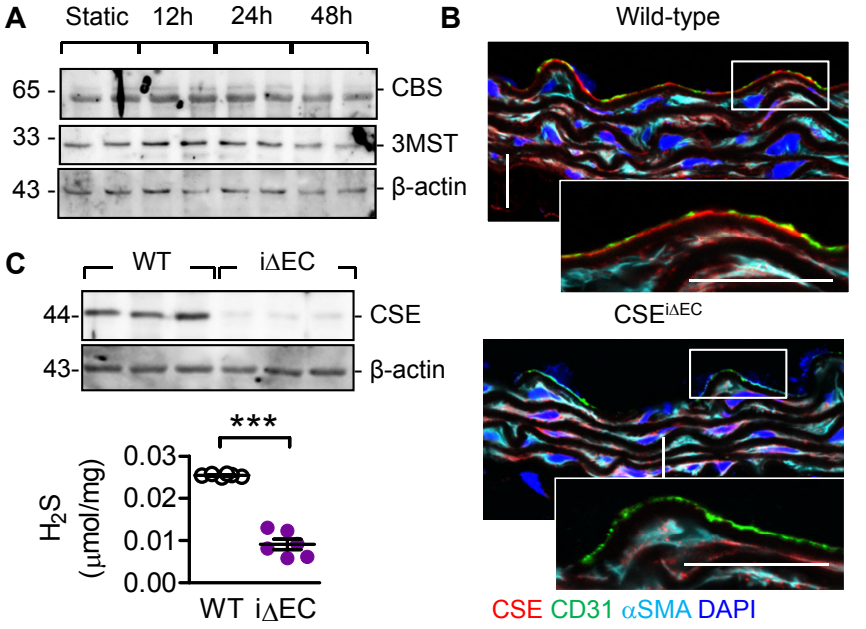

Supplemental Figure 1. **Effect of shear stress on CBS and 3MST levels and effect of endothelial CSE deletion in H_2S production. A**| CBS and 3MST levels in cultured endothelial cells exposed to fluid shear stress (12 dynes/cm^2) for up to 48 hours. Representative Western blot of additional 5 independent experiments of human endothelial cells (ANOVA, Newman-Keuls). **B**| CSE (red), CD31 (green) and α-smooth muscle actin (SMA; cyan) in cross sections of aortae from wild-type and CSE$^{i\Delta EC}$ mice; bar = 20 μm. Comparable images were obtained in samples from 5 additional animals per genotype. **C**| Expression of CSE in (upper panel), and generation of H_2S by (lower panel) endothelial cells from wild-type (WT) and CSE$^{i\Delta EC}$ (iΔEC) mice, n=6 animals per group (Student's t test). ***P<0.001.

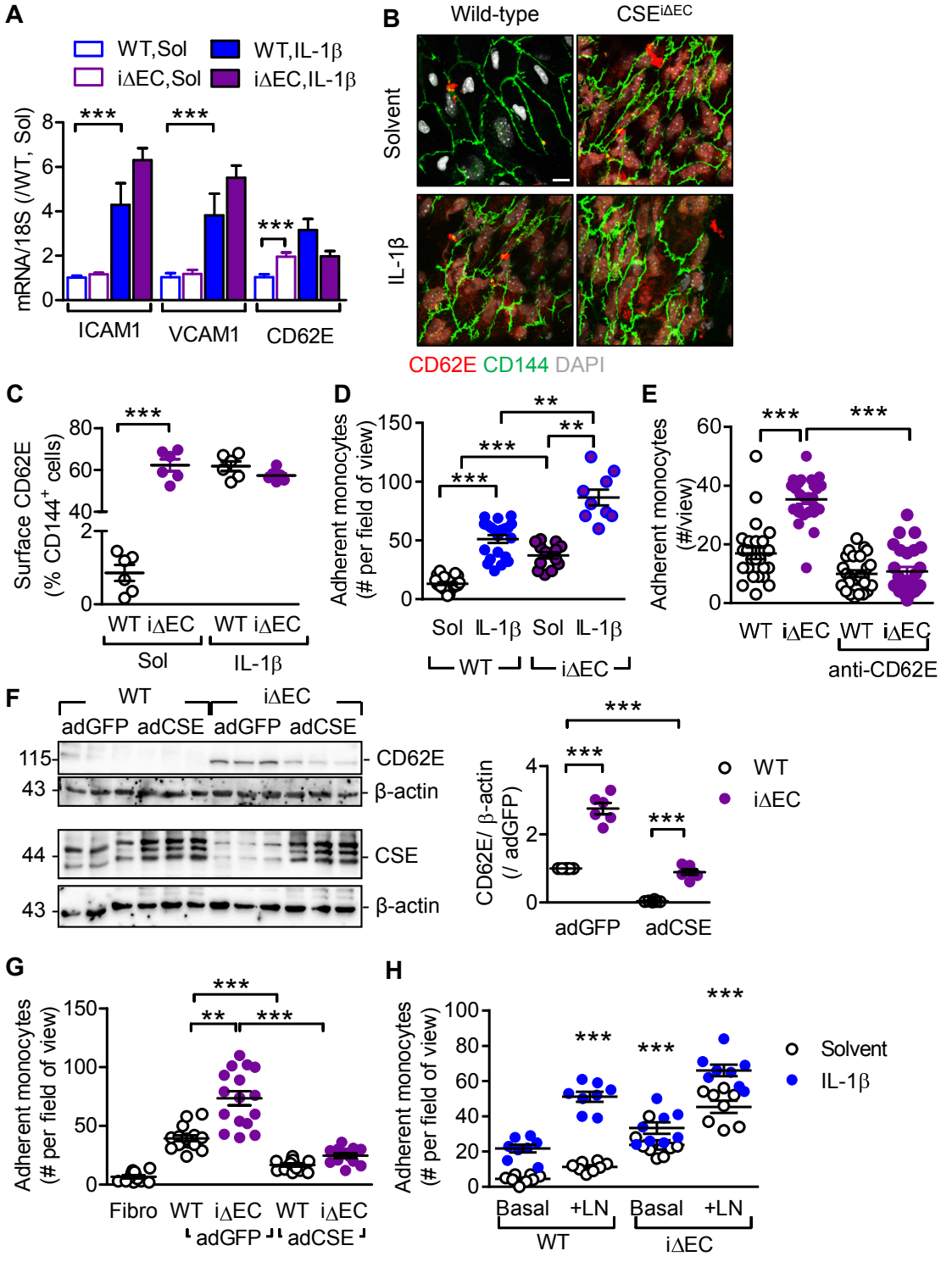

Supplemental Figure 2. **Consequences of CSE deletion on monocyte adhesion. A**| Pulmonary endothelial cells were isolated from wild-type (WT) and CSE$^{i\Delta EC}$ (iΔEC) mice and stimulated with solvent or IL-1β (30 ng/ml) for 3 hours. mRNA levels of ICAM1, VCAM1 and CD62E in cells treated with Sol or IL-1β (30 ng/ml, 3 hours). The graphs summarize n=6-9 experiments from 6 different batches of endothelial cells (ANOVA, Newman-Keuls). **B**| *en face* staining of CD62E (red) and CD144 (green) in descending aortae from wild-type and CSE$^{i\Delta EC}$ mice. Similar results were obtained using 5 additional animals per group. **C**| Surface expression of CD62E in cultured endothelial cells from wild-type and CSE$^{i\Delta EC}$ mice, n=6 different cell batches (2 way ANOVA , Bonferonni). **D**| Adherence of THP-1 monocytes to endothelial cells from wild-type (WT) and CSE$^{i\Delta EC}$ (iΔEC) mice treated with solvent (Sol) or or IL-1β (30 ng/ml) for 3 hours. n=6-9 experiments from 6 different batches of endothelial cells (ANOVA, Newman-Keuls). **E**| Adherence of monocytes to endothelial cells from wild-type (WT) and CSE$^{i\Delta EC}$ (iΔEC) mice in the absence and presence of a CD62E neutralizing antibody, n=6 experiments each performed in triplicate or quadruplicate using 6 different cell batches (2 way ANOVA , Bonferonni). **F**| CD62E expression in endothelial cells from wild-type (WT) and CSE$^{i\Delta EC}$ (iΔEC) mice after transduction with adenoviruses encoding GFP (adGFP) or CSE (adCSE), n=6 experiments using 6 different endothelial cell batches (ANOVA, Newman-Keuls). **G**| Monocyte adherence to endothelial cells from wild-type (WT) and CSE$^{i\Delta EC}$ (iΔEC) mice following transduction with adGFP or adCSE. Adherence on fibronectin (Fibro) was included as a negative control, n=6 experiments (each in duplicate or triplicate) using 6 different endothelial cell batches (ANOVA, Newman-Keuls). **H**| Adherence of monocytes to endothelial cells from wild-type (WT) and CSE$^{i\Delta EC}$ (iΔEC) mice and treated with solvent or IL-1β (30 ng/ml, 3 hours). Experiments were performed in the presence of L-sepiapterin (10 µmol/L) and in the absence (Basal) and presence of L-NAME (+LN; 300 µmol/L); n=6 experiments using 3 different endothelial cell batches (2 way ANOVA, Bonferonni). $^{**}P<0.01$, $^{***}P<0.001$.

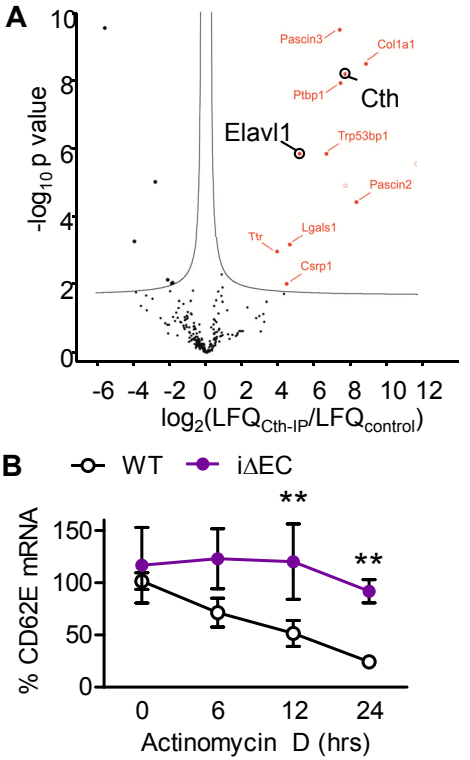

Supplemental Figure 3. Identification of the CSE interactome and link to CD62E mRNA stability. **A**| Volcano plot showing proteins co-precipitated with CSE (Cth); Elavl1= HuR. **B**| CD62E mRNA levels in wild-type (WT) and $CSE^{i\Delta EC}$ (iΔEC) endothelial cells following incubation with actinomycin D (1μg/ml), n=6 experiments using 4-6 different cell batches (2 way ANOVA, Bonferonni). $^{**}P<0.01$.

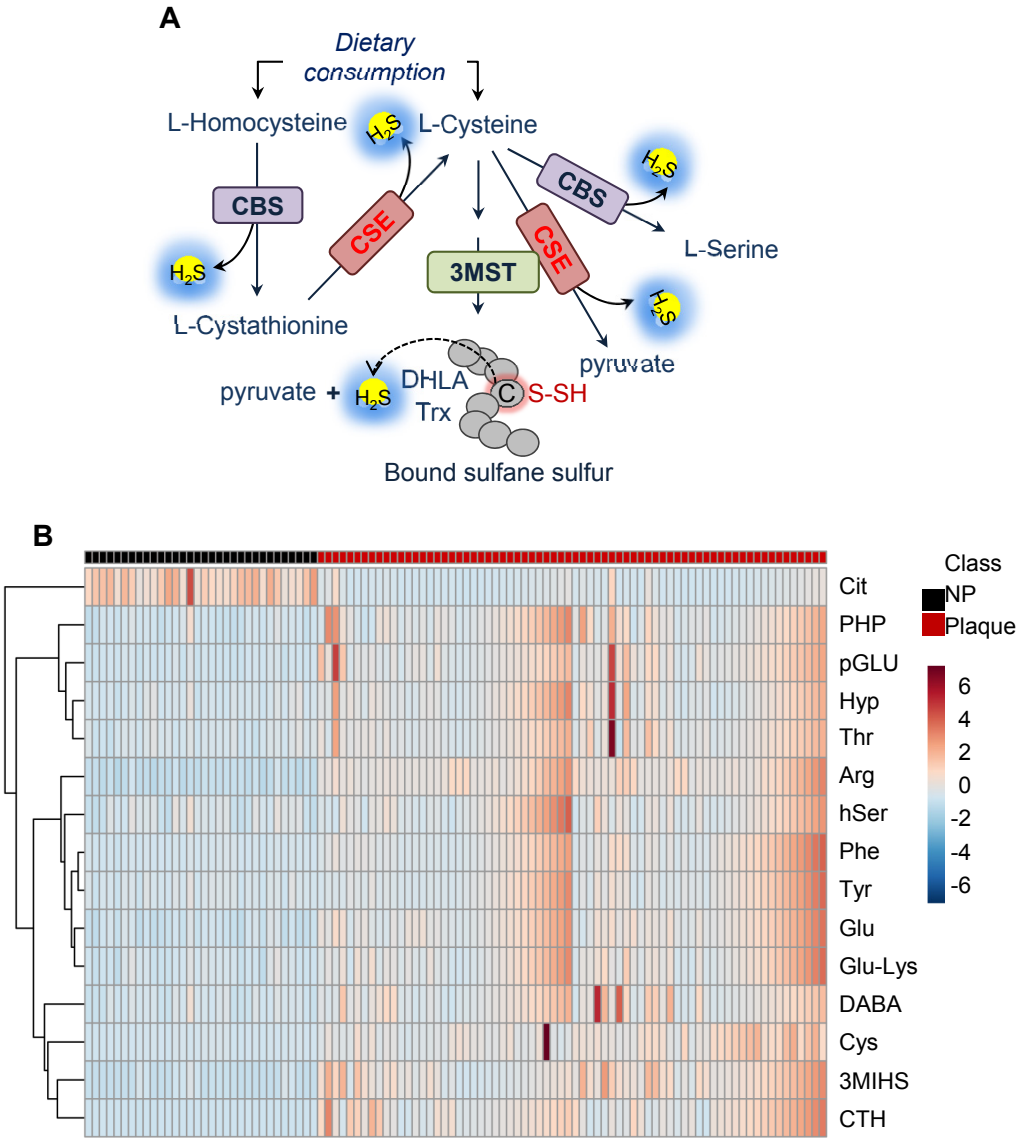

Supplemental Figure 4. **CSE substrate bioavailability in human samples. A**| L-Cysteine metabolism in mammalian cells. CBS catalyzes β-replacement of homocysteine and L-cysteine to produce L-cystathionine, H_2S and L-serine. CSE catalyzes the hydrolysis of L-cystathionine and L-cysteine. 3-MST produces bound sulfane sulfur from 3-mercaptopyruvate, which is generated from L-cysteine by aminotransferase (CAT). Thioredoxin (Trx) and dihydrolipoic acid (DHLA) are endogenous reducing cofactors that facilitate the release of H_2S from 3MST. **B**| Hierarchical clustering analyses of the top 15 plasma amino acids from the human cohort studied. The color key indicates the average fold change, blue: lowest; red: highest, n=102 plasma samples.

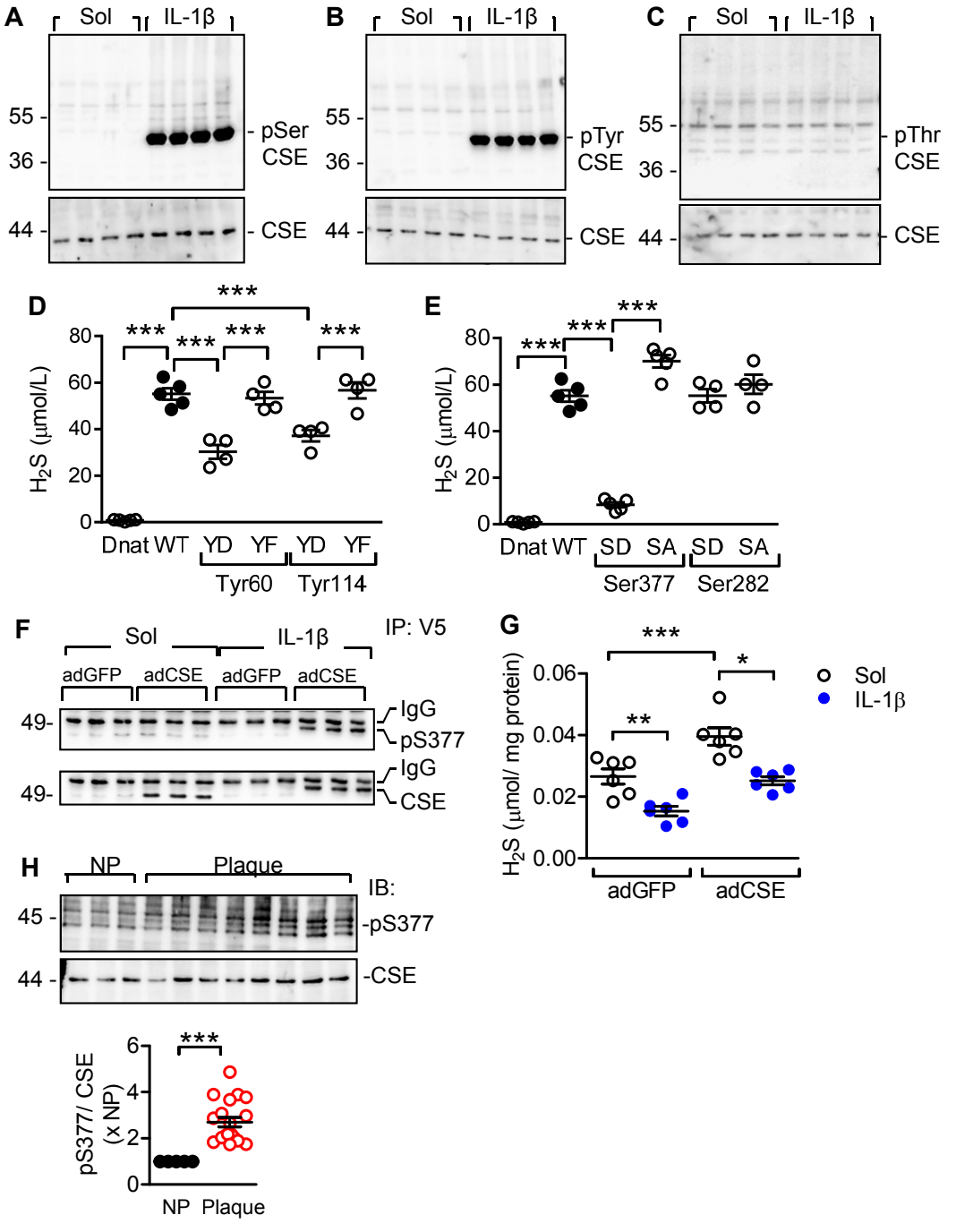

Supplemental Figure 5. **CSE phosphorylation on Ser377 and its consequences on CSE activity during inflammation. A-C**| Human endothelial cells were treated with solvent or IL-1β (30 ng/ml) for 18 hours. CSE was immunoprecipiated and immunobloting was performed using antibodies directed against phospho-serine (A), phospho-tyrosine (B) and phospho-threonine (C). The results are representative of experiments performed using 4 different cell batches. **D-E**| H_2S production *in vitro* by the wild-type CSE as well as the Tyr60 and Tyr144 mutants (D) and Ser377 and Ser282 mutants (E) assessed using the methylene blue assay. A denaturated wild-type CSE (Dnat) was used as negative control, n=4-5 independent experiments (ANOVA, Newman-Keuls). **F**| CSE phosphorylation on Ser377 in human endothelial cells transduced with adGFP or adCSE and treated with solvent (Sol) or IL-1β, n=6 different cell batches. **G**| H_2S production by the cells shown in panel h , n=6 independent cell batches (ANOVA, Neuman-Keuls). **H**| CSE phosphorylation on Ser377 in samples from non-plaque ateries (NP; n=5) versus atherosclerotic plaques (n=20; Mann Whitney). *P<0.05, **P<0.01, ***P<0.001.

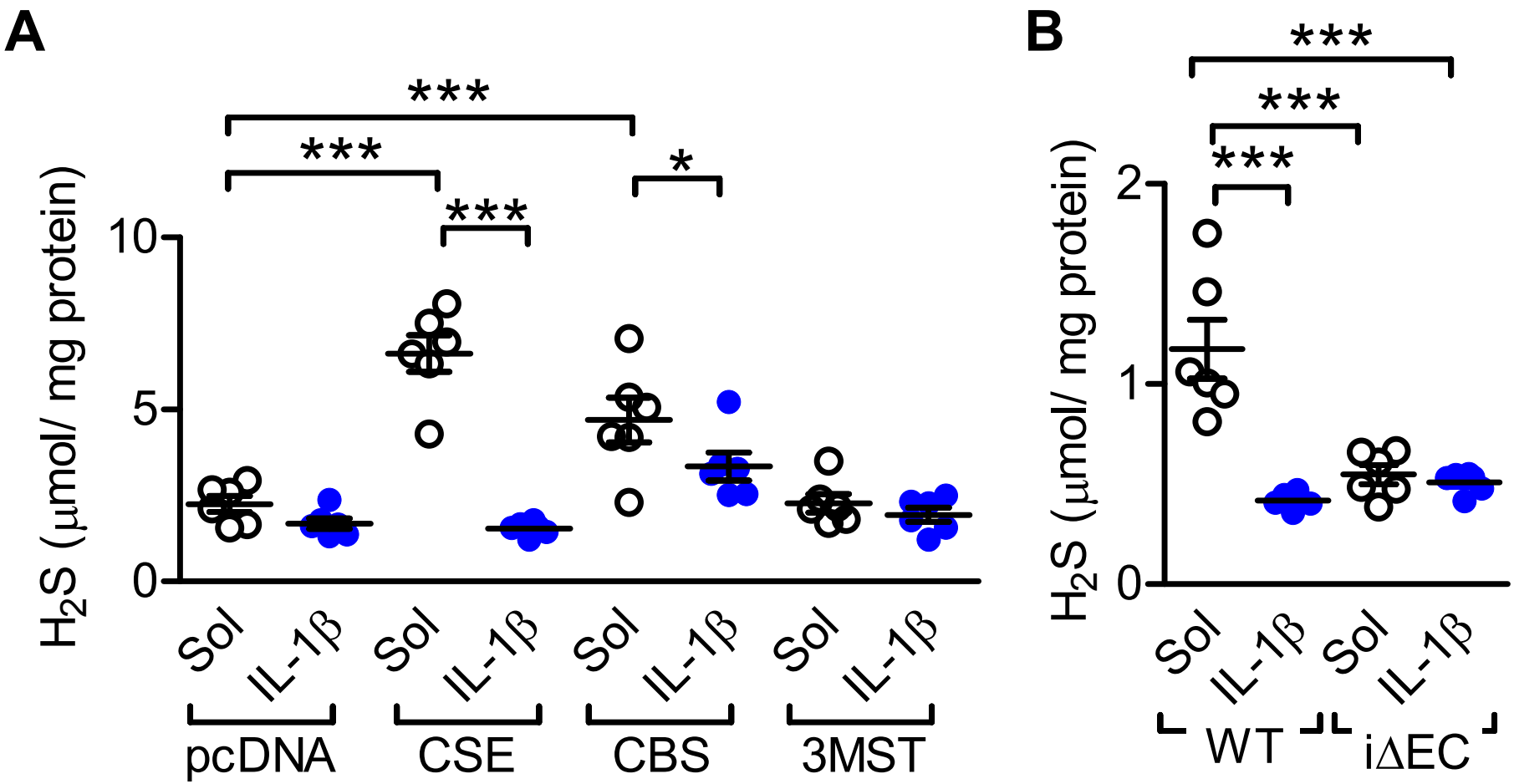

Supplemental Figure 6. **Effects of inflammation on CBS and 3MST.** **A|** Effect of IL-1β (30 ng/ml, 18 hours) on H_2S production by HEK-293 cells transfected with an empty vector (pcDNA), CSE, CBS or 3MST, n=5 independent experiments, (ANOVA; Newman-Keuls). **B|** Effect of IL-1β (IL, 30 ng/ml, 18 hours) on H_2S production by endothelial cells from wild-type (WT) and $CSE^{i\Delta EC}$ mice; n=6 independent experiments each using a different cell batch (ANOVA; Newman-Keuls). *P<0.05, ***P<0.001.

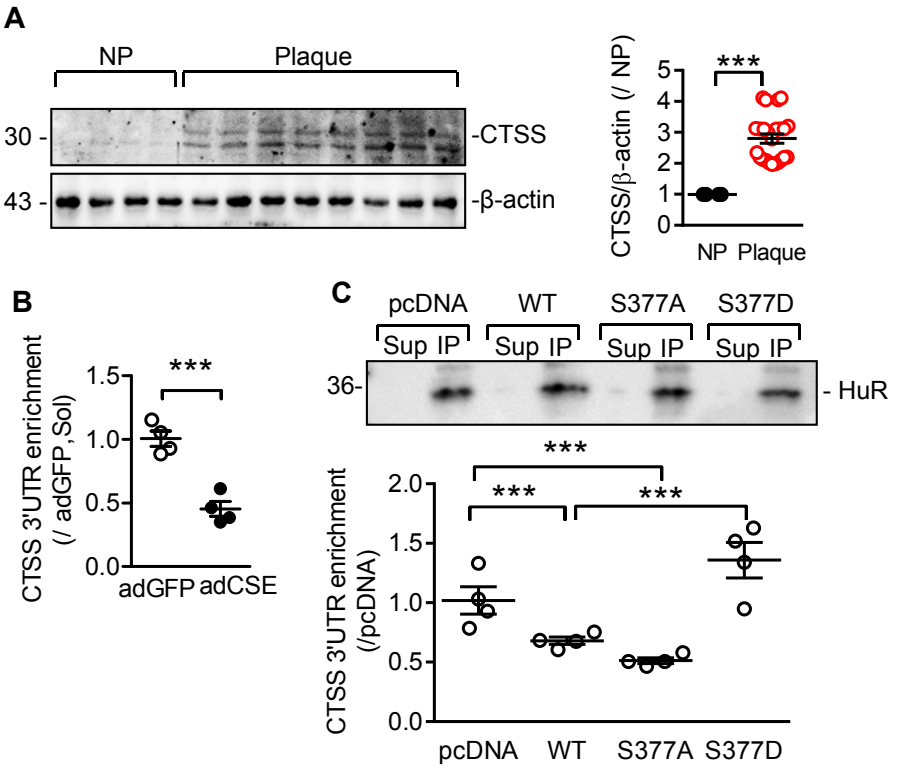

Supplemental Figure 7. Link between HuR sulfhydration in human plaques and CTSS levels and link between CSE activity and HuR RNA binding capacity. A| CTSS expression in non-plaque (NP) material as well as in atherosclerotic plaques from human subjects. **B|** Levels of *CTSS* 3'UTR RNA co-precipitated with HuR from human endothelial cells, n=4 different cell batches (Students's t test). **C|** CTSS RNA immunoprecipitated from HEK cells transfected with an empty vector or CSE wild type and mutant plasmids, n=4 experiments using 4 different cell batches (ANOVA, Newman-Keuls). The blots demonstrate the equivalent immunoprecipitation (IP) of HuR and are representative of 3 additional experiments. Sup = supernatant after IP. ***P<0.001.

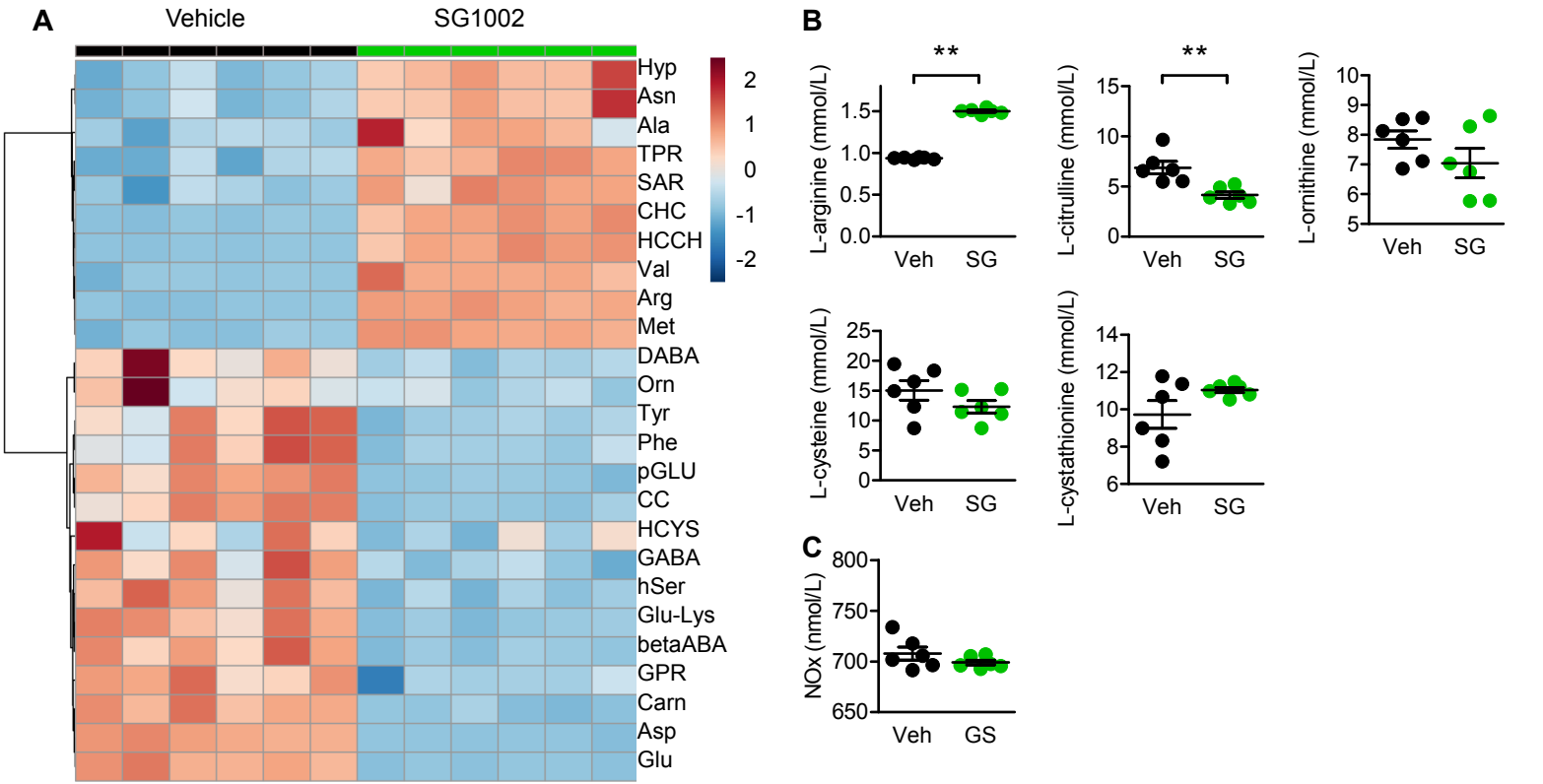

Supplemental Figure 8. Effect of SG1002 on circulating amino acid and nitrite levels. A| Hierarchical clustering analyses of (the top 25) amino acids in plasma from ApoExCSE$^{\Delta EC}$ mice after carotid ligation and treated with vehicle (Veh) or SG1002 (SG) for 21 days. The colour key indicates metabolite average fold change, blue: lowest; red: highest. **B|** Circulating levels of L-arginine, L-citrulline, L-ornithine, L-cystathionine and L-cysteine, n=6 animals per group (Mann Whitney). **C|** Nitrite levels (NOx, as a readout of NO availability) in plasma from the same mice studied in panel B. **P<0.01

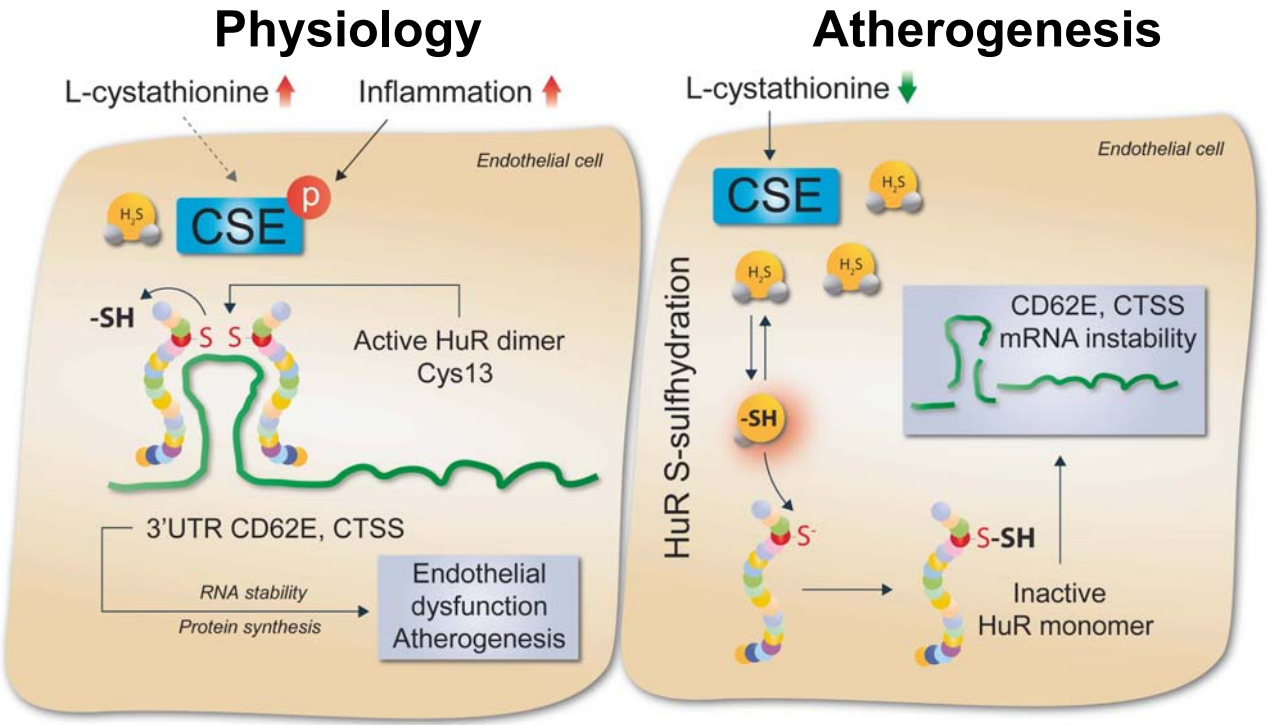

Supplemental Figure 9. Graphical abstract. In physiological conditions circulating L-cystathionine is metabolized by cystathionine gamma lyase (CSE) to generate intracellular H_2S. At physiological pH more than 80% of H_2S is in its ionic form (HS^-) which attacks the highly nucleophilic Cys13 of the RNA binding protein HuR to preserve its monomeric form and maintain its activity low, leading to increased instability of the target mRNAs i.e. *CD62E* and *CTSS*. This results in the preservation of endothelial function in atheroprone regions. However, in the presence of excessive circulating pro-inflammatory cytokines, CSE is phosphorylated on S377 and inhibited. L-cystathionine is elevated in the circulation, whilst intracellular and circulating H_2S levels are rapidly reduced. The absence of H_2S and subsequently HS^- allows the formation of the disulfide bond in Cys13 and homodimeritation of HuR. The HuR dimer exerts increase activity and elevated capacity to bind to the target 3´UTRs leading to increased stability of the *CD62E* and *CTSS* mRNAs, elevated protein synthesis and further development of endothelial dysfunction coupled with an enhanced and accelerated pro-atherogenic phenotype.